

Master's Programme in Advanced Energy Solutions

Technoeconomic comparison of Variable-Speed and Fixed-Speed Compressors in Hydrogen Pipeline Transport

Abdul Ahad

Copyright ©2025 Abdul Ahad

Author Abdul Ahad

Title of thesis Technoeconomic comparison of Variable-Speed vs. Fixed-Speed Compressors for Hydrogen Pipeline Transport

Programme Advanced Energy Solutions

Major Sustainable Energy systems and Markets

Thesis supervisor Prof. Anouar Belahcen

Thesis advisor(s) Dr. Juha Saari

Date 26.05.2025

Number of pages 60

Language English

Abstract

This thesis explores the techno economic analysis of two compression strategies employed in a 1,500 km long hydrogen pipeline. Using realistic hourly demand and variable compressors modelled in python and pipeline hydraulics to account for realistic pressure drops, this study contrasts variable-speed compressors without storage with fixed-speed compressors in conjunction with large geological storage. Despite an 8% increase in CAPEX, variable-speed drives reduce compression energy by ~20%, saving €45-47 M/year in electricity and levelized compression costs by 15–20%, according to integrated pipeline hydraulics and compressor performance modelling. Sensitivity analyses demonstrate additional cost savings through booster spacing optimization and operating below peak flow. Because variable-speed compression eliminates storage requirements and speeds up inverter pay-back, it performs better overall than fixed-speed systems.

Keywords Variable speed drives (VFD), constant speed compressor, hydrogen, pipeline, LCOH, Friction factor

Table of contents

Preface and acknowledgements	5
Abbreviations	6
1 Introduction	7
2 Hydrogen Pipeline System and Compression Technologies	9
2.1 Critical factors in hydrogen transport and compression	10
2.2 Gas pipeline fundamentals	12
2.3 Hydrogen compression technologies	15
2.3.1 Fixed and variable speed compressor operation	19
2.3.2 Commercially available VFDs offered by industries	21
2.4 Cost analysis for hydrogen compressors	23
2.5 Hydrogen storage	26
3 Modelling the Hydrogen pipeline	29
3.1 Variable speed Compressor Performance Model	29
3.2 Gas flow and pressure drop	33
3.3 Economical model	35
3.4 Load data and assumptions	36
3.5 Energy consumption comparison model	38
4 Case Study: A 1500KM Hydrogen Transmission Pipeline	40
4.1 Input parameters	41
4.2 Test 24-hour variable load profile	42
4.3 Energy consumption comparison for variable Industrial load	46
4.4 LCOH results	47
4.5 Sensitivity of changing maximum flow rate	48
4.6 Sensitivity of changing Number of enroute stations and spread distance	50
5 Conclusion	54
References	56
APPENDIX	60

Preface and acknowledgements

I wish to express my deepest gratitude to Professor Anouar Belahcen and my advisor, Juha Saari, for their invaluable guidance and unwavering support throughout this thesis.

My sincere thanks also go to Janne Grönlund and Mari Tuomaala for generously sharing their expertise and providing crucial insights. Finally, I am profoundly grateful to my family and friends for their constant encouragement and support.

Otaniemi, 26 May 2025

Abdul Ahad

Abbreviations

H ₂	Hydrogen
EHB	European Hydrogen backbone
km	Kilometer
FS	Fixed-Speed (compressor)
VSD	Variable-Speed Drive (compressor)
CAPEX	Capital Expenditure
OPEX	Operating Expenditure
O&M	Operation and Maintenance
TCI	Total Capital Investment
LCOH	Levelized Cost of Hydrogen
API	American Petroleum Institute
STP	Standard Temperature and Pressure
NIST	National Institute of Standard and Technology
DB	Darcy Weisbach (pressure-drop model)
CFD	Computational Fluid Dynamics
SciPy	Scientific Python library
M	Million (e.g., “€45 M”)
€/kg H ₂	Euro per kilogram of hydrogen
VFD	Variable-Frequency Drive
SoB	Safety On Board
CSD	Constant-Speed Drive
TACCS	Turbo-Air Centrifugal Compressor System
IGV	Inlet Guide-Vanes
V/f	Voltage-to-Frequency ratio
DTC	Direct Torque Control
FOC	Field-Oriented Control
STO	Safe Torque Off
PID	Proportional Integral Derivative (controller)
HFC	Hydrogen Fuel-Cell
COP	Coefficient of Performance
LH ₂	Liquid Hydrogen
LOHC	Liquid Organic Hydrogen Carrier
MOF	Metal-Organic Framework
kW	Kilowatt
kWh	Kilowatt-hour
Mt	Megatonne
Nm ³ /h	Normal cubic meters per hour

1 Introduction

The global transition toward low-carbon energy is providing momentum for the rapid expansion of renewables with wind and solar power, yet their intermittent nature and seasonal mismatch continue to disrupt grid stability. Hydrogen comes in as a very versatile energy carrier if one investigates storing surplus renewables, giving high-temperature heat to industrial processes, and smoothing short-term fluctuations in power supply. The contrast of its high gravimetric energy density, about 120 MJ/kg, against its exceptionally low volumetric energy density, around 0.01 MJ/L (seen in Figure 1) at atmospheric conditions, demands that highly pressurized pipelines and specialized compression systems be utilized for its efficient transport over long distances. [1]

While there are many similarities between natural gas and hydrogen pipeline networks, there are also some differences. For example, the low density and small molecular size of hydrogen increase the risk of diffusivity and leakage, and embrittlement issues necessitate careful material selection and monitoring. Additionally, compressor stations, which are typically operated at fixed speed with throttling control, suffer significant energy penalties under variable load because throttling dissipates excess power rather than optimizing machine performance [2]. There is a lack of guidance for infrastructure planning and operation because the techno economic feasibility of alternative compression strategies like integrating variable-speed drives (VSDs) to adjust compressor speed in real-time remains understudied under realistic, time-varying demand profiles. Several studies done on techno economics of gas pipelines suggest that compressors can account for 15 – 30 % of total CAPEX of pipeline and compression energy dominates OPEX. [3] [4]

In this thesis an integrated simulation model is used to assess the life cycle costs and energy consumption of two hydrogen pipeline compression configurations: variable-speed compression without dedicated storage and fixed-speed compression with supplemental storage. To capture hourly variations in flow, pressure drops, and compressor efficiency, this model combines real-gas pipeline hydraulics, compressor performance maps, and an economic evaluation framework. The study aims to provide a comprehensive understanding of how each strategy functions under actual operating conditions by fusing segment-by-segment pressure-drop calculations with empirical performance data.

This thesis's main goals are to compare the life cycle costs including capital expenditure, operating expenses, and storage investment of both compression strategies over a yearlong consumption profile and to quantify the operating energy savings achieved when switching from fixed-speed compressors (augmented by storage) to variable-speed compressors that dynamically match demand.

The thesis is structured as follows. Chapter 2, reviews hydrogen's thermo-physical properties, pipeline flow modelling, compressor technologies including fixed- and variable-speed drives and economic considerations for compression and storage Chapter 3 describes the simulation methodology, which includes cost analysis, load profiling, pipeline hydraulics, and compressor performance modelling along with test runs to verify the working of the models; The configuration for a case study of 1,500 km transmission pipeline under an hourly varying load is set and input parameters for the comparison model are presented in Chapter 4. Chapter 5 summarizes the results and makes recommendations for operational strategies and compressor selection as well as future research directions.

2 Hydrogen Pipeline System and Compression Technologies

Hydrogen transmission pipelines closely mirror today's natural gas networks. At the inlet, a large electric motor compressor, either a reciprocating piston or a centrifugal unit pressurizes the gas into the transmission range, and smaller booster stations spaced every 100 - 500 km keep the line pressure between 30 and 100 bar. Alongside these compressor sites, buffer storage typically underground salt caverns at 55 - 150 bar or above-ground high-pressure vessels at 100 - 200 bar hold hundreds to thousands of tons of hydrogen. By absorbing daily and seasonal swings in supply and demand, this storage reduces compressor cycling and maintains a steady, reliable flow. Figure 1 represents such a pipeline model. [5]

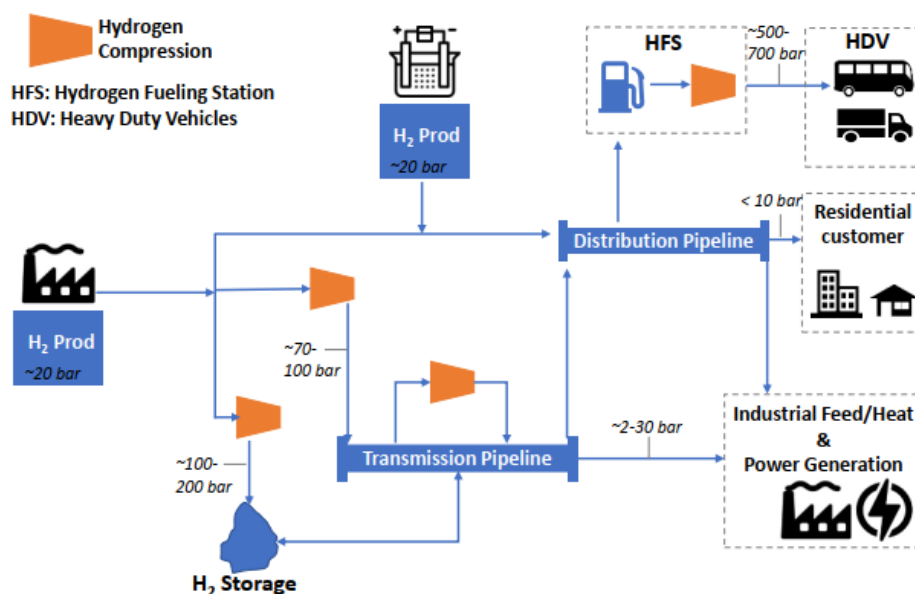


Figure 2. Schematic showing future H₂ gas pipeline transportation system

From a central control room, operators can adjust compressor output, open or close valves and isolate line sections remotely, while city-gate regulators step pressure down to 2 - 30 bar for distribution and end-use needs. [3]

Despite these engineering controls, hydrogen embrittlement remains the chief integrity challenge. High-strength steels (> 5200 bar) are prone to crack initiation at weld heat-affected zones, so designers favour lower-strength grades (≤ 3600 bar) or derate operating pressures when higher grades are unavoidable. Distribution mains in many countries already use API 5L A/B/X42-X46 steels, which under typical pressures show negligible

embrittlement, and permeation through polyethylene service lines is also economically acceptable for lower-pressure networks. [6]

2.1 Critical factors in hydrogen transport and compression

In developing an effective hydrogen pipeline network, several critical properties of hydrogen significantly influence both pipeline design and operational management.

Because hydrogen has a very low density and a high buoyancy (approximately 0.0899 g/L at STP) [7], pipelines must either have a larger diameter or operate at much higher pressures in order to transport the same amount of energy as denser gases. Because of its small molecular size and high diffusivity, hydrogen is more likely to permeate metals and seals. Without hydrogen-specific materials or improved gaskets, valves and welds could become potential leakage points, requiring continuous, high-sensitivity leak-detection systems to ensure safety and reduce environmental impact [3], [4]. Hydrogen embrittlement adds to these design difficulties because atomic hydrogen can permeate conventional steel and cause microcracks that weaken the material's mechanical integrity. Operators usually choose lower-strength pipeline steels (such as X52 or lower grades) to reduce embrittlement.

The thermophysical properties of hydrogen have an additional impact on operational plans. Its high thermal conductivity ($\approx 0.1807 \text{ W/m}\cdot\text{K}$) helps dissipate heat generated during compression or frictional flow, easing thermal-management requirements, and its low kinematic viscosity ($\approx 8.76 \times 10^{-6} \text{ m}^2/\text{s}$) reduces frictional losses and yields efficiency gain [3], [6]. However, hydrogen deviates from ideal-gas behavior at high pressures required to counteract its low volumetric energy density ($\approx 0.01 \text{ MJ/L}$ at STP compared to 0.0378 MJ/L for methane) as seen in Figure 2.

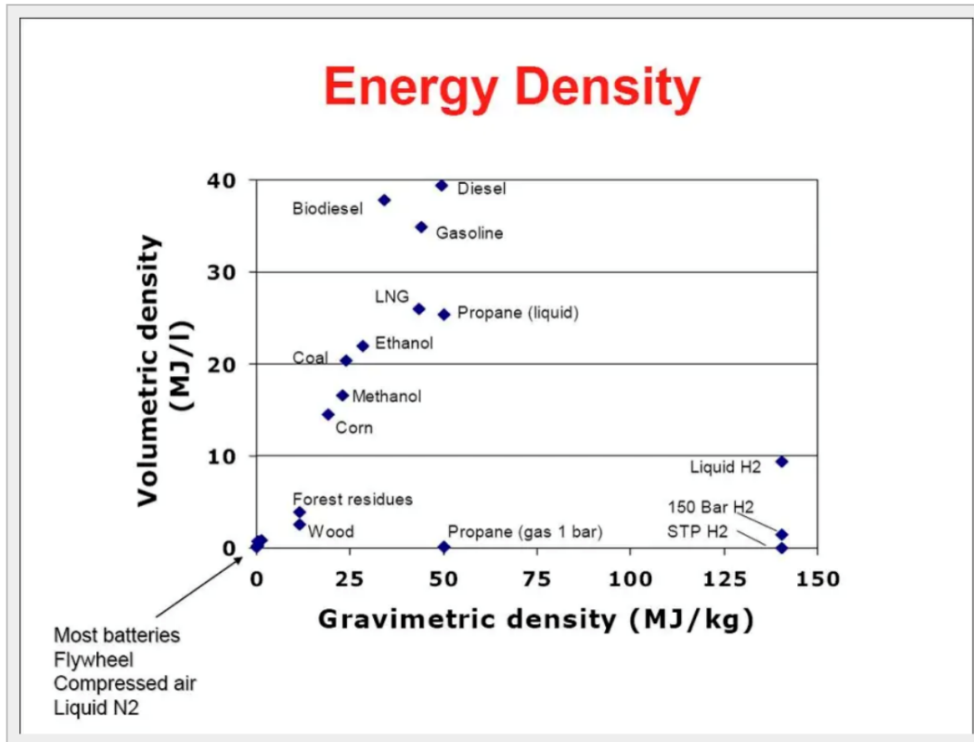


Figure 3. Energy density comparison of different fuels [1]

The compressibility factor (Z) can vary from roughly 0.98 to 1.3, depending on temperature and pressure conditions (see Figure 3), and must be precisely accounted for using tools like NIST REFPROP or CoolProp to prevent miscalculating flow and compression work [7][8].

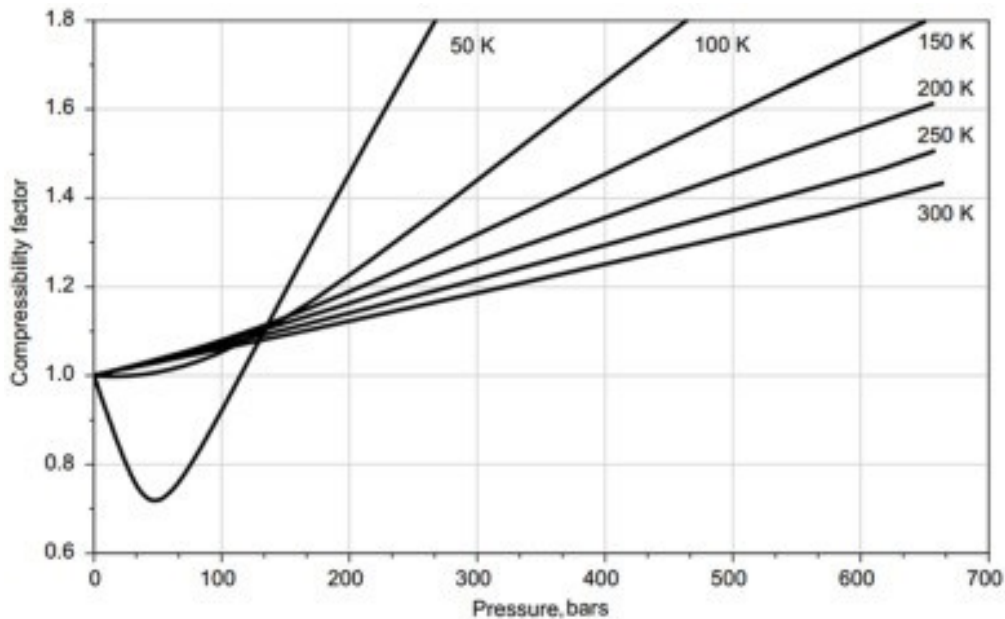


Figure 4. Hydrogen compressibility factor chart at different temperature and pressure

A thorough understanding of these properties ensures safe, efficient, and economically viable transport of hydrogen gas.

2.2 Gas pipeline fundamentals

In hydrogen pipelines, the driving force for flow is the pressure differential between inlet and outlet, and the rate at which pressure drops along the line is governed by both the gas's thermophysical properties and the pipe's hydraulic resistance. For a steady, isothermal, single-phase flow as shown in Figure 4.

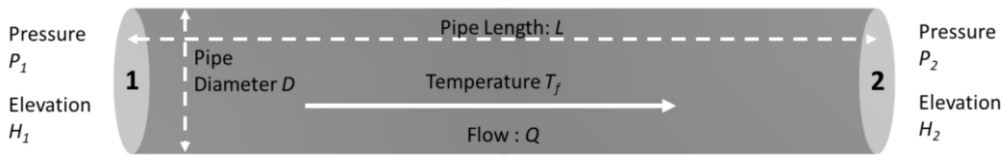


Figure 5. Steady state flow in a gas pipeline

The generalized flow equation can be written in the form:

$$Q = 1.1494 \times 10^{-3} \left(\frac{T_b}{P_b} \right) \left[\frac{(P_1^2 - e^s P_2^2)^{0.5}}{f G T_f L_e Z} \right] D^{2.5} \quad (1)$$

- L is pipe length in km.
- S is an elevation adjustment parameter and is dimensionless as defined in Eq. 2.
- L_e is equivalent pipe length in km as defined by Eq. 3.
- D is inside pipe diameter in mm.
- P_1 is inlet pressure in kPa (Absolute pressure, not gauge pressure)
- P_2 is outlet pressure in kPa (Absolute pressure, not gauge pressure)
- P_b is base pressure in kPa (101.352 kPa = 1.01352 bar).
- T_b is the base temperature in K (288.706 K).
- T_f is the average flowing temperature of gas in K.
- G is specific gravity (For Hydrogen, $G = 0.0696$)
- Z is the compressibility factor at average temperature and pressure.
- f is friction factor and is dimensionless

$$s = 0.0684G \left(\frac{H_2 - H_1}{T_f Z} \right) \quad (2)$$

Where in the above equation H_1 and H_2 are inlet and outlet elevation in meters.

$$L_e = L \left(\frac{e^s - 1}{s} \right) \quad (3)$$

The study done in the technical report on hydrogen pipeline suggests that if we target a fixed outlet velocity we can use Eq 1 to calculate pressure drop and eventually p_2 using a loop as shown in Figure 5.

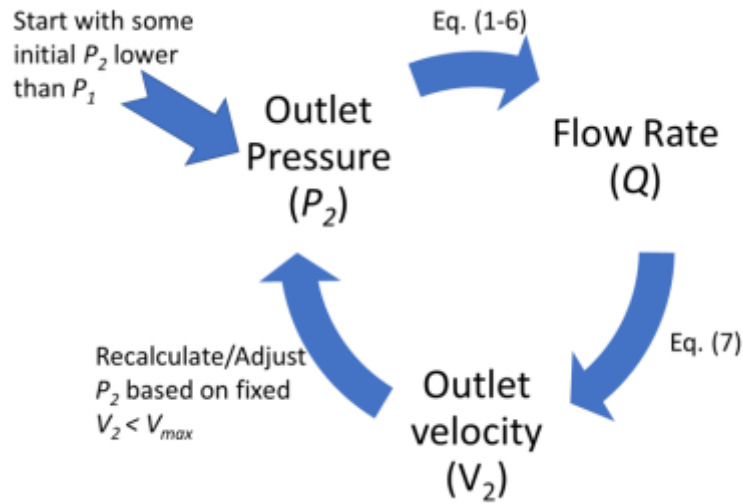


Figure 6. Method to calculate outlet pressure in H2 pipeline [6]

Other equations used in the calculation are as follows:

$$p_{avg} = \frac{2}{3} \left(\frac{p_1^3 - p_2^3}{p_1^2 - p_2^2} \right) \quad (4)$$

Average pressure is the average of initial and final pressure at two ends of the pipeline segment e.g if initial pressure is 70 bar than p_1 is 70 bar while p_2 on the other end will be approximately 28 bar [3].

$$Re = \frac{D \rho_{avg} V_{avg}}{\mu} \quad (5)$$

Equation 5 gives us the Reynolds number which tells us if the flow is laminar ($Re < 2,000$) or turbulent ($Re > 4000$). In most gas pipelines the flow is turbulent.

$$\frac{1}{\sqrt{f}} = -2 \log_{10} \left(\frac{\varepsilon}{3.7 D} + \frac{2.51}{Re \sqrt{f}} \right) \quad (6)$$

Equation 6 is used to calculate Darcy friction factor f iteratively.

$$V = 14.734 \left(\frac{P_b}{T_b} \right) \left(\frac{ZT}{P} \right) \left(\frac{Q}{D^2} \right) \quad (7)$$

Eq 7 gives us the velocity of gas in pipeline which is inversely proportional to pressure level. Research material and methods

- V_{avg} is average gas velocity in m/s.
- D is inside pipe diameter in m.
- μ is gas viscosity in kg/ms.
- V is gas velocity in m/s.
- Q_b is gas flow rate in Sm³/day.
- D is inner diameter of pipe in mm.
- P_b is base pressure in kPa (101.352 kPa).
- T_b is the base temperature in K (288.706 K).
- P is gas pressure in kPa.
- T is the gas temperature in K.
- G is Gas gravity and is dimensionless.
- Z is compressibility factor at pipeline conditions and is dimensionless.
- ϵ is pipe roughness in mm
- ρ_{avg} is average gas density in kg/m³.

where 1 kPa = 0.01 bar.

Although this method gives reasonable results, it is still hard on computation as two loops get involved. First is the main loop as shown in figure 5 and second is the inner loop to find friction factor f . While equation 6, also called Colebrook white equation is used to find the value of f iteratively using an initial value of Re and f as it cannot be solved explicitly.

Instead of that we can use equation 8 also called as Darcy Weisbach equation directly to eliminate the outer loop as done in a separate study done by Fraunhofer Institute for Factory Operation and Automation IFF. [8]

$$\Delta p = f \frac{L}{D} \rho \frac{v^2}{2} \quad (8)$$

This study from IFF demonstrated that dividing the pipeline into very fine sections (on the order of 1 km) and recalculating density, Reynolds number,

and friction factor in each segment drives cumulative error below 1 %, with only a modest additional computational cost compared to coarser segmentation. Taken together, these papers show that while quick algebraic formulas are useful for early estimates, the gold standard for predicting hydrogen outlet pressure remains a real gas, segment by segment Darcy Weisbach framework.

The segment method has also been endorsed in the study done by Thawani et al. (2023). Who took a classic segment-by-segment approach based on the Darcy Weisbach equation, pairing real-gas compressibility and viscosity data from CoolProp with an iterative Colebrook White solution for friction factor. When they compared their analytical results against a $k - \epsilon$ CFD model, the two methods agreed within about 5 % over a range of steel and polymer pipe cases, confirming that a well-tuned “textbook” approach can rival more computationally intensive simulations. [9]

2.3 Hydrogen compression technologies

Hydrogen compression technologies (compressors) fall into two broad mechanical categories (see Figure 6) positive-displacement machines that squeeze a fixed volume of gas, and dynamic machines that impart velocity to the flow each suited to various parts of a pipeline network.

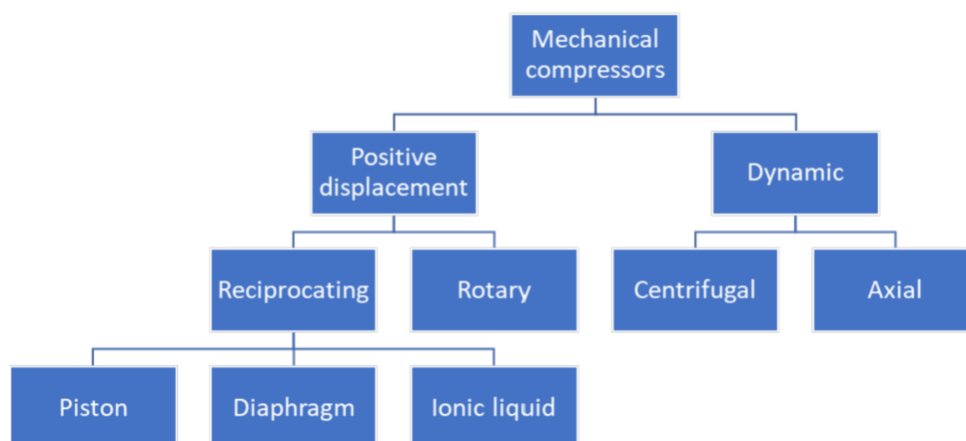


Figure 7. Types of mechanical compressors

In most large-scale transmission and booster stations, multi-stage reciprocating piston compressors (as the one seen in Figure 7) remain the workhorse, with power ranging from 300 kW to 18,000 kW [10]. In these units, one or more pistons cycle back and forth in cylinders, trapping a fixed charge of hydrogen and progressively raising its pressure through successive stages. Modern oil-free designs have achieved discharge pressures up to 850 bar

from 350 bar in two or three stages, with flow capacities as high as 5,084 Nm³/h in the largest installations. Their biggest advantage is the ability to reach extremely high pressures in relatively few stages (a 4:1 pressure ratio can be done in two piston stages rather than six centrifugal stages). On the other hand, these machines require complex sealing systems, frequent piston-ring replacements, and careful thermal management since, without oil lubrication, component temperatures can spike under heavy load.

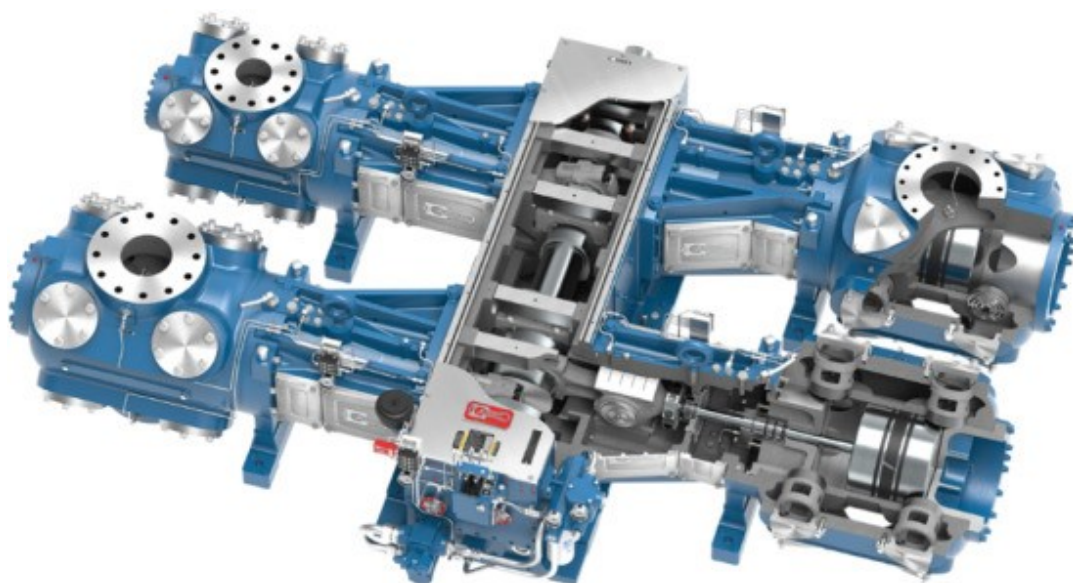


Figure 8. Structure of a large multistage reciprocating compressor [11]

For applications requiring ultra-pure hydrogen at moderate pressure such as fuelling stations or specialty industrial processes metal-diaphragm compressors offer a seal-less alternative. Here a hydraulic fluid presses on a thin, corrugated metal diaphragm, isolating the gas chamber from the drive mechanism. With clever head designs, companies like PDC Machines and Howden have built diaphragm units capable of single-stage pressure ratios rivalling multistage pistons: up to 517 bar discharge in one head, and even 1,000 bar with just two stages from a 50 bar inlet.

When exceptionally large volumes at moderate pressures (30-100 bar) are needed such as in the main transmission line itself centrifugal compressors dominate. A high-speed impeller accelerates hydrogen, and a downstream diffuser converts that velocity into pressure. Because hydrogen's density is 1/14th that of natural gas, tip speeds must climb to roughly 700 m/s, driving the use of advanced titanium alloy wheels and tight tolerances to avoid surge and choke limits. Per stage pressure ratios hover around 1.2:1, so multistage trains with intercooling are the norm, delivering up to 50,000 Nm³/h in a

single unit (seen in Figure 8) with isentropic efficiencies near 80 %. While centrifugal machines have fewer moving parts and lower vibration than pistons, their aerodynamic complexity and tip speed requirements make them costly to engineer and maintain. [11]

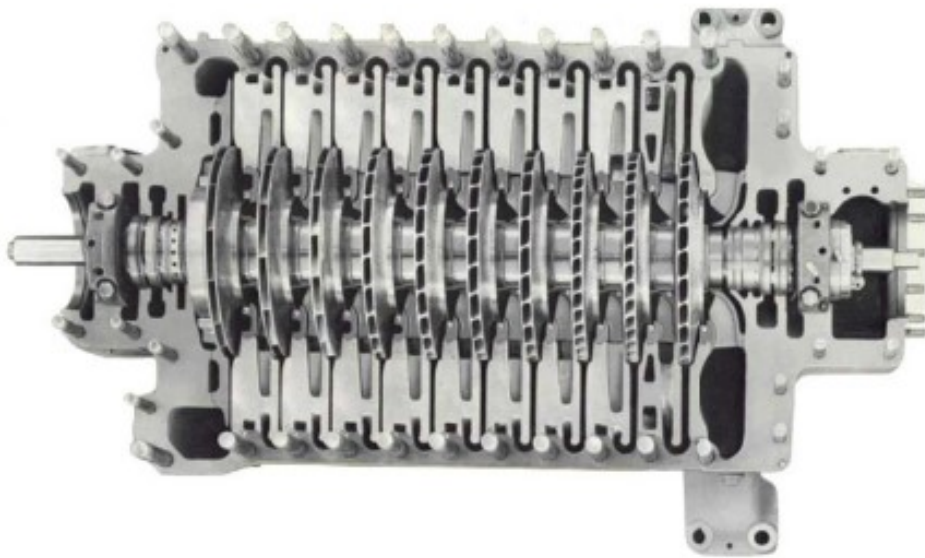


Figure 9. Cutaway of a multistage centrifugal compressor

Engineers visualize this behaviour of compressor with a compressor performance map, plotting normalized flow on the horizontal axis against pressure ratio on the vertical axis as shown below in Figure 9. A family of “constant speed” curves sweeps upward and rightward from low flow and low-pressure ratio each curve corresponding to a fraction of the machine’s maximum shaft speed. At the far left of each curve, a dashed “surge line” marks the boundary where reverse flow and pressure pulsations begin, operating too close to surge risks mechanical damage. To the right lies the “choke line,” beyond which the impeller cannot further accelerate the fluid, capping maximum flow. Superimposed on this picture are efficiency islands roughly oval contours that show, for example, 80 %, 75 % and 70 % isentropic efficiency. The sweet spot for energy-efficient operation sits near the peak of these islands on the 100 % speed curve, and engineers size and stage compressors to keep normal pipeline flows within or just to the left of that peak.

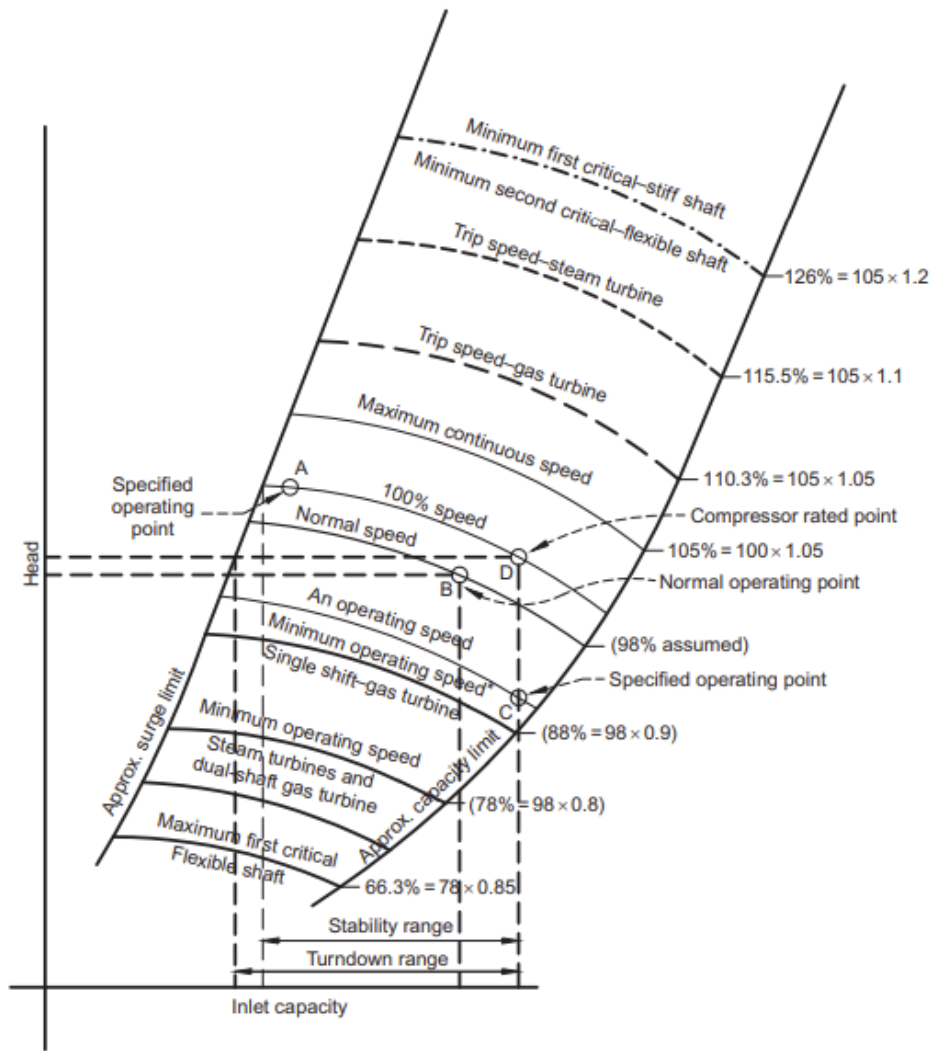


Figure 10. Typical centrifugal compressor performance map. Courtesy of the American Petroleum Institute [12]

Centrifugal compressors in hydrogen service do not just rely on raw mechanical design and exotic materials they also lean on “affinity” or “fan” laws to predict how slight changes in shaft speed will affect flow, pressure and power.

Performance for speeds other than the rated speed can be estimated from the following equations:

$$\frac{Q_1}{Q_2} = \frac{N_1}{N_2} \tag{9}$$

$$\frac{H_1}{H_2} = \left(\frac{N_1}{N_2}\right)^2 \tag{10}$$

$$\frac{HP_1}{HP_2} = \left(\frac{N_1}{N_2}\right)^3 \quad (11)$$

In their simplest form, these scaling relationships tell us that volumetric flow is directly proportional to rotational speed ($Q \propto N$), the pressure “head” generated by an impeller scale with the square of speed ($H \propto N^2$), and the power required climbs with the cube of speed ($HP \propto N^3$). This means, for example, spinning the shaft 10 % slower will cut flow by about 10 % but trim power draw by roughly 27 % a powerful incentive for variable-speed operation.

The model in this thesis also makes use of the affinity laws in the calculation of compressor work calculation for variable speed compressor operation.

2.3.1 Fixed and variable speed compressor operation

Fixed speed (or constant speed) and variable speed compressors represent two fundamentally different approaches to matching compressor output with process demand. Traditional fixed-speed compressors, driven directly by electric motors or gas turbines, operate at a single design speed. They rely on flow control devices throttling valves, inlet guide vanes (IGVs), or blow off valves to regulate discharge pressure and flow. While mechanically simple, this on/off or load cycling control incurs significant energy losses whenever demand deviates from the design point. In a turbo air centrifugal compressor system (TACCS), for example, precise pressure control via IGV trimming is effective but wastes energy: a constant speed drive (CSD) forces the motor and impeller to run continuously at full speed, generating large electrical and mechanical losses when throttled.

By contrast, variable speed compressors integrate a variable frequency drive (VFD) or variable-speed drive (VSD) between the power supply and motor. A simple VFD operational diagram can be seen in Figure 10.

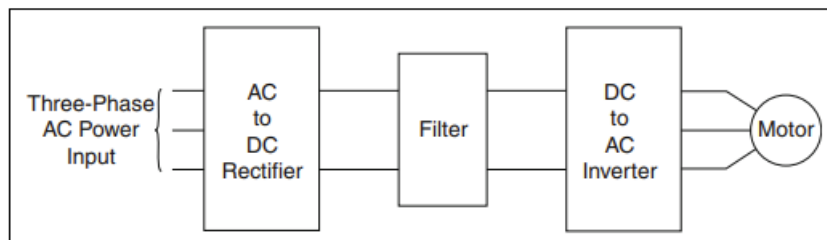


Figure 11. Variable frequency drive operational diagram

This inverter modulates motor speed and thus compressor impeller tip speed so output pressure and flow can be adjusted at the source, rather than by choking flow downstream. The affinity laws dictate that reducing motor speed by x % cuts power draw by roughly x^3 %, so even modest speed reductions yield outsized energy savings. In one study of a 1,000 hp turbo centrifugal compressor, replacing the CSD + IGV control with a quadratic V/f VSD scheme improved system efficiency by over 23% and reduced electrical losses by 4.44% under part-load conditions, with payback on the inverter investment in under three years. [13]

Across refrigeration, heat pump and industrial air compression applications, VSD equipped compressors routinely outperform fixed-speed counterparts:

1. In refrigerated display cabinets, variable speed (DC + inverter) compressors achieved a total daily energy consumption of 8.3 kWh which is 25.9 % lower than the fixed-speed (AC, on/off) system. [14]
2. In residential heat pumps using scroll compressors, a two-stage variable speed compressor (VSC) architecture raised coefficient of performance (COP) by 37.6 % versus single speed operation. [15]
3. An industrial case showed 24.3 % energy savings over the full load profile and an estimated USD 207 k cost benefit over the warranty period for a VSD retrofit on a turbo-air centrifugal compressor. [16]

Beyond energy efficiency, VFDs offer softer starts (limiting inrush currents), finer control bandwidth (via PID or more advanced controls), and reduced mechanical stress extending equipment life. Harmonic mitigation measures (line reactors, passive/active filters, multi-pulse rectifiers) address power-quality concerns in modern VFDs, making them reliable for sensitive industrial environments. [17]

While fixed speed compressors remain viable for high duty, constant load duties, variable speed drives unlock significant energy and operational benefits in variable load contexts. The upfront inverter cost typically pays back in 1 to 3 years through energy savings alone, making VFDs an increasingly standard choice in new and retrofit compressor installations.

2.3.2 Commercially available VFDs offered by industries

At present, several VFD manufacturers offer compressor-specific drives well suited for hydrogen fuel cell (HFC) air compressors, even though none yet explicitly market them under the HFC label. The data below, drawn from recent industry surveys, can guide the selection of drives for HFC compressor applications.

ABB

The ABB ACS880 family ranges from 0.55 kW up to 6,000 kW and, based on the power required, operates on voltages from 230 V to 690 V. While ACS5000 is designed for high-power industrial applications and ranges from 2MW to 36MW. These drives provide sub-3 % harmonic distortion with ultra-fast torque response through ABB's trademarked Direct Torque Control (DTC) technique, and boast a high level of efficiency (98.5%) with regenerative capabilities built in. [18]

Siemens

The SINAMICS G120X by Siemens has been the number one choice for pumps, fans, and compressors operating within a power range of 0.75-630 kW on 400-690 V with frequency/conversion (V/f), field oriented control (FOC), and sensorless vector control with built in Safe Torque Off (STO). For truly heavyweight and servo applications, the SINAMICS S120 ranges between 0.55 and 9,000 kW on 380–690 V.[19], [20]

Danfoss

The VLT Automation Drive FC 301/302 series by Danfoss sweeps from 0.25 kW to 1.4 MW on 200-690 V, with no derating from -25 °C to 50 °C. The drives use Smart Logic Control to relieve CPUs of tasks; back channel cooling to prolong electronics life; plug in modules for rapid commissioning; and energy optimization algorithms, being highly wear resistant and favored in continuous duty compressor and industrial air handling applications.[21]

Rockwell Automation

Rockwell's PowerFlex 755 covers the range from 0.75 kW to 1.5 MW at 200/240 V, 380/480 V, and 600/690 V, V/Hz, sensor-less vector, and DTC control options. Having embedded Safety On Board (SoB), EtherNet/IP motion integration, and modular I/O. At the top of the line, the 755T ranges from 1.5 to 2.6 MW across the same voltage classes. [22], [23]

Yaskawa

The A1000 drive of Yaskawa gives powers on the range of 1,000 HP (about

750 kW) at voltages 200-690, having V/f, closed-loop vector, and DTC for controls.[24]

Schneider Electric

Schneider's Altivar Process ATV 600 targets fluid and gas handling from 0.55 – 1,600 kW on 380-480 V with V/f and sensor-less vector plus embedded energy monitoring and fieldbus support. For larger plants, the ATV 900 covers 11–3,550 kW on 400 - 690 V with FOC, sensor-less vector, advanced diagnostics, functional safety options (STO, SS1). [25], [26]

Mitsubishi Electric

Mitsubishi's FR-F800 series, comprising the FR-F800-E version, offers pump/fan oriented controls, energy saving features, low-speed high-torque capability, and light-duty or super light-duty user-selectable modes. The capacity of the drives ranges from 0.4 kW to 1.6 MW at 200-690 V, and they make V/f control possible, as do superlative PID loops and optional embedded Ethernet communications for compressor application-side ease of integration and performance monitoring.[27]

Fuji Electric

Fuji's FRENIC-Mega drives (FRN015G1S-4U) take 200-480 V input and give out 500 Hz max, having inverter efficiencies of 96-98%. Dynamic base-voltage set-up, real time current monitoring for peak efficiency, embedded energy consoles, a plethora of digital I/O all these make the drives manageable within small packaging and offer high switching frequency options suitable to high-precision compressors and air-separation services in hydrogen and petrochemical plants.[28]

Table 1. Manufacturer and product parameters of dedicated VFD for air compressors

Manu- facturer	Key Series / Models	Supply Voltage (V)	Power Range (kW)	Control Method(s)
ABB	ACS880 sin- gle/drive modules	230 - 690	0.55 - 6000	Direct Torque Control (DTC), V/f, vector con- trol
	ACS5000	6,000 - 13,800	2,000 - 36,000	Direct Torque Control (DTC); 36-pulse diode rectifier
Sie- mens	SINAMICS G120X	400 - 690	0.75 - 630	V/f, field-oriented con- trol (FOC), sensorless vector
	SINAMICS S120	380 - 690	0.55 – 9,000	Field-oriented/servo control; ultra-fast

				torque response; MindSphere predictive maintenance
Danfoss	VLT-FC 301/302	200 - 690	0.25 - 1400	V/f, flux-vector control, torque control
Rockwell Automation	PowerFlex 755 / 520	200/240 - 600/690	0.75 - 1500	V/Hz, sensorless vector, Direct Torque Control (DTC)
	PowerFlex 755T	200 – 900	1.5 – 2,600	Direct Torque Control (DTC), sensorless vector
Yaskawa	A1000, V1000	200 - 690	0.4 - 710	V/f, closed-loop vector control, DTC
Schneider Electric	Altivar Process / ATV 600	200 - 690	0.55 - 1600	V/f, sensorless vector
	ATV900	400 - 690	11 – 3,550	Field-oriented control, sensorless vector
Mitsubishi Electric	FR-F800, FR-A800	200–690	0.4–1600	V/f, closed-loop vector control
Fuji Electric	FRENIC Mega / FRENIC ACE	200–690	0.4–1500	V/f, sensorless vector

2.4 Cost analysis for hydrogen compressors

The simple cost analysis calculation method is presented in the technical brief on hydrogen compression by transition accelerator team of Canada. It follows simple economic relations to find Capex, Non-energy OPEX and Energy cost which is used later to find the Lifecycle cost of hydrogen.

The study assumes parameters presented in Hydrogen delivery Scenario model (HDSAM) while the currency used is US dollar. In our calculations the costs will be calculated in euros using an appropriate conversion ratio as shown in Table 2. Compressors with variable speed control will consume less energy and will result in less electricity cost at part load conditions unlike fix speed compressor which has to run at design capacity.

1) Capex:

$$Capex_{comp} \left[\frac{Euro}{kgH_2} \right] = \frac{Annualized\ TCI \left[\frac{Euro}{yr} \right]}{Availability[\%] \times DesignCapacity \left[\frac{kg\ H_2}{day} \right] \times 365 \left[\frac{days}{yr} \right]} \quad (12)$$

The detailed method to get to capex is explained in technical brief of hydrogen compression [2].

The annual operating cost of a hydrogen compressor is split into energy (electricity) costs and non-energy OPEX (labor plus fixed O&M). Each component can be expressed as follows:

2) Energy/Electricity costs

Assuming we use electric motors as prime movers for our compressor machine, the cost of electricity can be calculated by multiplying the compressor power / work done by operating hours and electricity price per kWh as follows.

$$Electricity\ cost \left[\frac{Euro}{yr} \right] = Compressor\ rating\ (kW) * Operating\ hours \left(\frac{hr}{yr} \right) * Electricity\ price \left(\frac{Euro}{kWh} \right) \quad (13)$$

$$Energy_{comp} \left[\frac{Euro}{kgH_2} \right] = \frac{Electricity\ cost \left[\frac{Euro}{yr} \right]}{Availability[\%] \times DesignCapacity \left[\frac{kg\ H_2}{day} \right] \times 365 \left[\frac{days}{yr} \right]} \quad (14)$$

In our model later we will use hourly data for compressor work done per hour, as theoretically in case of variable load profile, the compressor with variable speed control will consume less energy and should result in less electricity cost at part load conditions unlike fixed speed compressor which has to run at design rating.

3) Non-Energy OPEX

Non-energy OPEX combines labour and fixed operations & maintenance:

$$Non - energy\ OPEX \left(\frac{Euro}{yr} \right) = Total\ labor \left(\frac{Euro}{yr} \right) + Fixed\ O\&M \left(\frac{Euro}{yr} \right) \quad (15)$$

While

$$Total\ labor\ \left(\frac{Euro}{yr}\right) = Direct\ labor\ \left(\frac{Euro}{yr}\right) + Indirect\ labor\ \left(\frac{Euro}{yr}\right) \quad (16)$$

Direct labor cost:

$$Direct\ labor\ \left(\frac{Euro}{yr}\right) = Annual\ labor\ hours\ \left(\frac{hours}{yr}\right) * Labor\ rate\ \left(\frac{Euro}{hour}\right) \quad (17)$$

$$Annual\ labor\ hours\ \left(\frac{hr}{yr}\right) = 288 * \left(\frac{x}{100,000}\right)^{0.25} \quad (18)$$

where x = compressor flow rate (kg H₂/day) and Labor rate = 33.9 Euro/hour for year 2024 [29]

$$Indirect\ labor\ \left(\frac{Euro}{yr}\right) = Direct\ labor\ \left(\frac{Euro}{yr}\right) * Indirect\ labor\ factor\ (\%) \quad (19)$$

Indirect labor factor = 50% used to consider the cost of overhead (i.e., head office, personnel) [2].

4) Lifecycle cost of hydrogen compression

A useful indicator of the relative economic viability of H₂ is the Levelized Cost of H₂ (LCOH). The simple definition of LCOH for compression is as follows:

$$LCOH_{comp} \left[\frac{Euro}{kgH_2}\right] = Capex_{comp} \left[\frac{Euro}{kgH_2}\right] + Non - energy\ OPEX_{comp} \left[\frac{Euro}{kgH_2}\right] + Energy_{comp} \left[\frac{Euro}{kgH_2}\right] \quad (20)$$

Apart from the compression cost, in the model used in this thesis we will use natural storage as well and include its cost when calculating the LCOH for the case of fix speed compressor scenario. For simplicity, only the compression cost of hydrogen will be considered for all sections of the model and not the decompression cost for distribution purposes.

Table 2. Economic assumptions for calculating LCOH for compression

Factor	Value	Source
Exchange rate	€ 0.924 / US\$	[30]
Inflation rate	e.g CAPEX from 2007 to 2024 = 800/525.4 = 1.5226	Chemical Engineering Plant Cost Index [31]

Discount rate	8%	[32]
Compressor lifetime	15 years	[2]
Electricity cost	€0.1867/kWh	[33]
Labor rate	€33.9/hr	[34]

2.5 Hydrogen storage

Hydrogen storage technologies fall into three broad categories physical, material based, and geological each offering a unique trade-off among capacity, cost, efficiency and application scale as summarized in Table 3. [35]

Physical storage

These methods include compressed gas, liquid hydrogen and chemical carriers. Today, most gaseous hydrogen is stored at 350 - 700 bar in composite or steel vessels; at 700 bar you can pack roughly 5 - 6 kg into a typical 150-liter tank, though cycle life and tank cost remain challenges [36]. Liquefied hydrogen (LH₂) boosts volumetric density by over a factor of ten compared to high pressure gas, but requires cryogenic cooling to -253 °C consuming up to 30 % of the hydrogen's energy content and incurring boil-off losses in transit or storage [37]. Chemical carriers such as ammonia or liquid organic hydrogen carriers (LOHCs) embed hydrogen in a liquid matrix, enabling ambient-temperature transport; the trade-off lies in the energy and capital cost of dehydrogenation at the point of use[38].

Material-based storage

This type leverages advanced solids metal hydrides, porous carbons, metal-organic frameworks (MOFs) and high entropy alloys to reversibly bind hydrogen at moderate pressures and temperatures. Metal hydrides like MgH₂ or LaNi₅ can achieve gravimetric capacities of 5-7 wt %, but heat management during (de)hydrogenation and cycling stability are main hurdles [24]. MOFs and activated carbons offer high surface areas for physisorption, with usable capacities near DOE targets at 77 K and 100 bar, yet performance drops sharply at ambient temperature unless pore chemistry is finely tuned. Recent first-principles studies on lithium-decorated nanoporous materials show promise for meeting volumetric targets at moderate pressures, underscoring the role of atomistic design in next-generation adsorbents.[38] .

Geological storage

Mostly referred to salt caverns provides bulk, long-duration buffering ideal for balancing seasonal renewables. Salt-cavern facilities operate at 55 - 150 bar, hold 500 - 6,000 t per cavern, and exceed 98 % cycle efficiency with negligible leakage, making them the proven large scale option [39].

Depleted gas fields and aquifers offer alternative reservoirs, though cushion-gas requirements and geochemical compatibility demand careful site evaluation [40].

Table 3. Comparison of hydrogen storage options

Category	Conditions	Typical Capacity	Advantages	Limitations
Physical				
Compressed gas	350 - 700 bar, ambient T	≈5 - 6 kg H ₂ per 150 L tank	Mature technology; fast fill/withdrawal	Low volumetric density; high-pressure equipment & safety needs
Cryogenic liquid (LH ₂)	-253 °C, ≈1 - 5 bar	≈70 kg H ₂ /m ³	High volumetric density; established handling	Liquefaction ~30 % energy penalty; boil-off losses
Chemical carriers (NH ₃ , LOHCs)	Ambient T and P	≈100 - 180 kg H ₂ /m ³ (carrier-dependent)	Liquid-tank transport; leverages existing infrastructure	Energy & capital cost of (de)hydrogenation; additional processing step
Material based				
Metal hydrides (e.g. MgH ₂ , LaNi ₅)	1 - 100 bar, 20 - 200 °C	40 - 150 kg H ₂ /m ³ ; 1 - 7 wt %	High volumetric density; safety of solid form	Slow kinetics; heat management during (de)hydrogenation; cycle degradation
Adsorbents (MOFs, activated carbon)	1 - 100 bar, 77 K (often)	30 - 60 kg H ₂ /m ³ (at 77 K & 35 - 100 bar)	Moderate conditions; tunable pore chemistry	Low ambient-T capacity; expensive materials; cryogenics often required
Geological				
Salt caverns	55 - 200 bar, ambient T	500 - 6,000 t H ₂ per cavern	Bulk, seasonal buffering; > 98 % round-trip efficiency	Site-specific geology; high upfront CAPEX; cushion-gas requirement

Despite these advances, no single storage method solves all needs. High-pressure tanks excel for mobility, liquid carriers fit long-haul transport, material based systems suit onboard or small-scale uses, and caverns underpin grid-scale buffering. Future research must drive down tank and hydride

costs, improve cycling stability of adsorbents, and expand geological storage capacity to meet projected hydrogen demands of 500 - 700 Mt by 2050 goals that will hinge on integrated storage solutions across all scales [41].

3 Modelling the Hydrogen pipeline

The purpose of the simulation model developed during this thesis is to measure and compare the energy consumption and costs of two types of hydrogen pipeline compression system, that is fixed-speed compressor operation and variable-speed compressor operation. In other words, it assesses energy savings and cost advantages that variable-speed drives could offer under realistic time-varying flow conditions.

3.1 Variable speed Compressor Performance Model

In this work, we developed a custom compressor performance module that leverages manufacturer-provided performance maps for centrifugal compressors (efficiency and speed lines) like the one shown in Figure 11. This map contains empirical data measured at several mass flow rates and rotational speeds, stored in CSV format. We take efficiency and mass flow data points from csv files. The datasets are then combined by employing multidimensional interpolation methods (LinearNDInterpolator and interp1d) to create continuous models of compressor performance as shown in workflow diagram in Figure 12. [42]

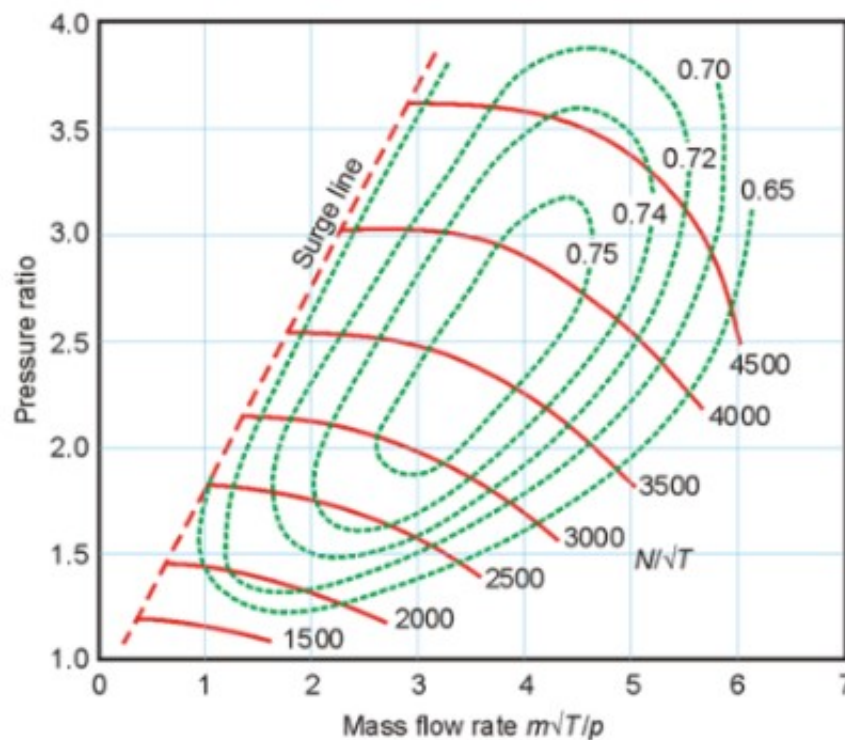


Figure 12. Typical centrifugal compressor map expressed in normalized mass and rotational speeds

By this technique, the simulation dynamically predicts the compressor axial speed and efficiency required at a given flow condition instead of assuming fixed values of compressor performance.

To test the compressor performance model, we simulate a random 24-hour varying load profile varying from 80% of design mass flow of 4kg/s to 100% randomly. This load profile accounts for fluctuations in hydrogen demand with respect to a nominal design flow rate of 4 kg/s. Every hour, the model calculates the power requirements, assuming both fixed and variable speed of operation. For the fixed speed, the compressor is said to be operating at a fix design point, and an average efficiency of 75% is assumed.

For the variable speed operation, the procedure dictates determining the necessary RPM to produce the desired pressure ratio, retrieving the efficiency for that speed from the interpolated map, and then scaling the power at the retrieved efficiency level by applying the affinity law as decried in section 1.4, which states that compressor power varies directly with the cube of rotational speed.

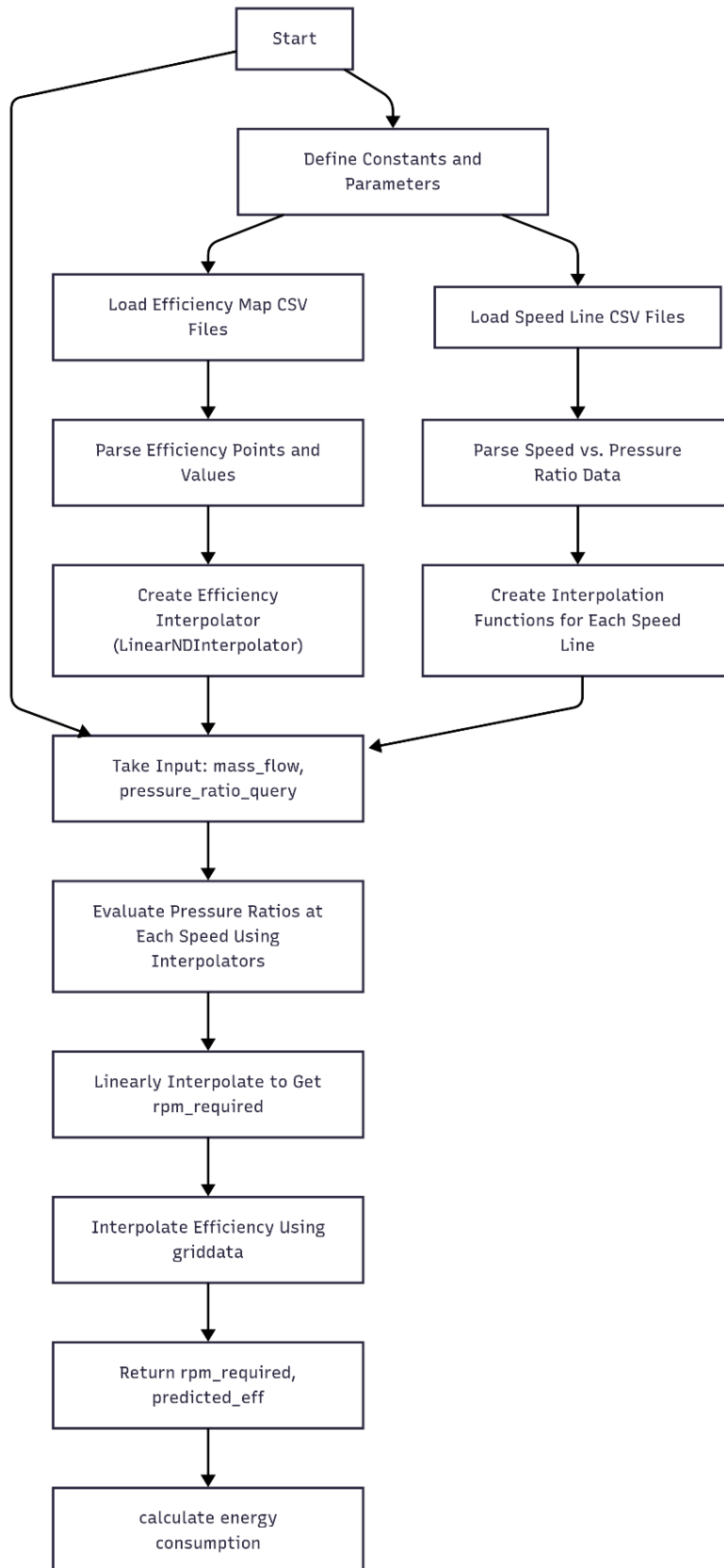


Figure 13. Workflow of compressor model test setup

Energy consumption by a multilevel compressor is calculated using standard isentropic work equation [11].

$$Power = N \left(\frac{k}{k-1} \right) \left(\frac{\dot{m}}{\eta} \right) T_{suc} R \left[\left(\frac{P_{disc}}{P_{suc}} \right)^{\left(\frac{k-1}{Nk} \right)} - 1 \right] \quad (21)$$

Figure 13 shows us that variable speed compressors adjust its rpm and efficiency each hour as required demand changes and required demand as a result the consumed energy seen in Figure 14 also varies each hour while for fix speed compressors it remains constant i.e. 11806kWh.

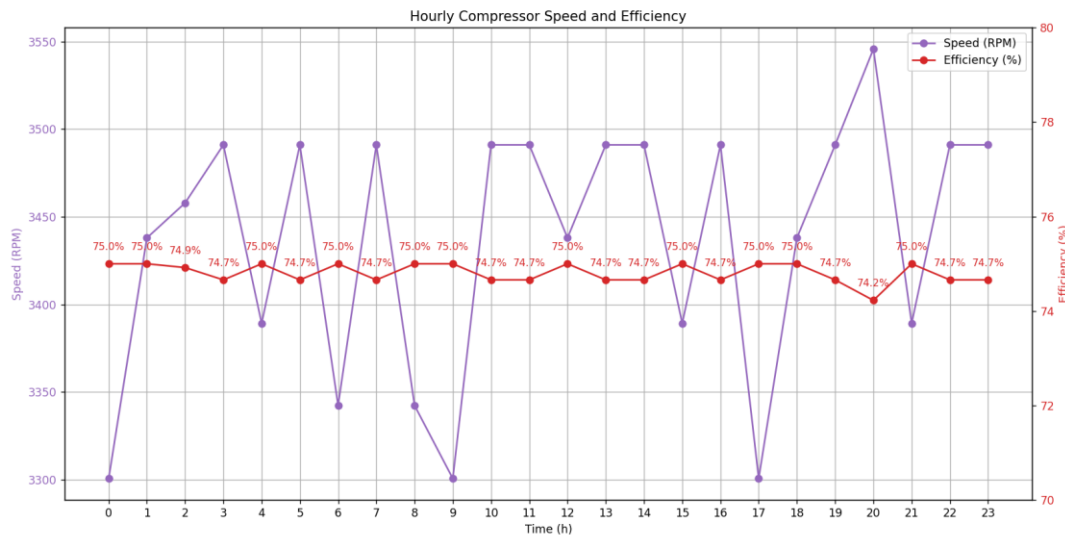


Figure 14. Variable speed and efficiency at different load conditions from the performance model

Although the overall savings are 13.17% for this profile but we can see that the affinity law can also amplify the energy consumption in overload conditions, i.e. the speed required for flow exceeds the design point, which was taken as 3600 rpm in this case.

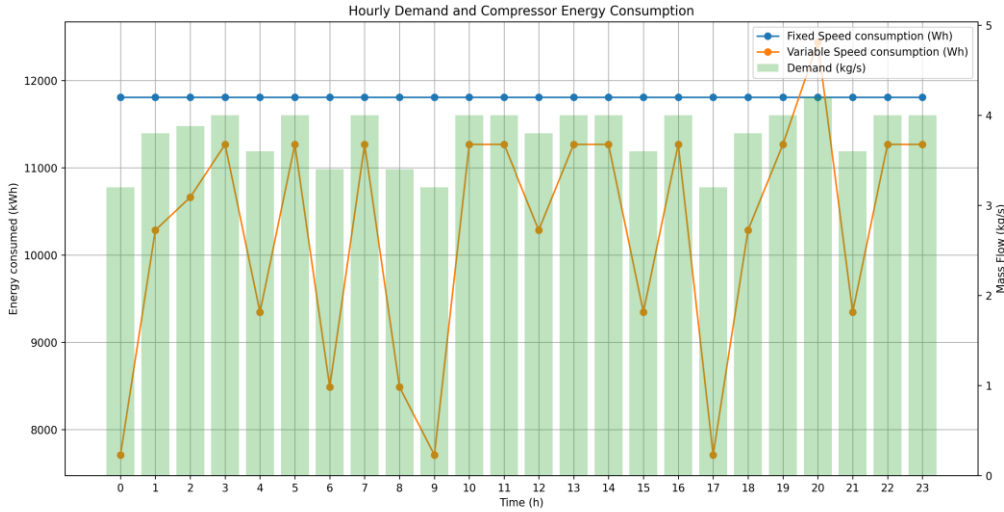


Figure 15. Energy consumption comparison

3.2 Gas flow and pressure drop

In this section, we have developed a custom pipeline pressure drop simulation workflow as shown in Figure 15. It is built on the segment-by-segment approach first described by IFF [8].

The pressure drop through a pipeline of hydrogen gas would be simulated by the model, given an inlet pressure and mass flow rate. The parameterization is based on a physically accurate method from fluid dynamics and real-gas behavior. The pipeline is divided into several smaller segments, and the parameters determining gas behavior: compressibility factor, dynamic viscosity, and density, are computed for each segment by the CoolProp library. Using the gas properties, we can determine the velocity and Reynolds number.

We then solve the Colebrook White equation via an implicit iterative routine to find the Darcy friction factor. Then, knowing the friction factor, we calculate the pressure drop over the pipe section using the Darcy-Weisbach equation and updates the inlet pressure for the next section. This way, when repeated over the full length of the pipeline, the model calculates the total pressure drop and then obtains the outlet pressure, allowing a highly detailed and accurate assessment of how hydrogen behaves in long distance pipeline transport systems under varied operating conditions.

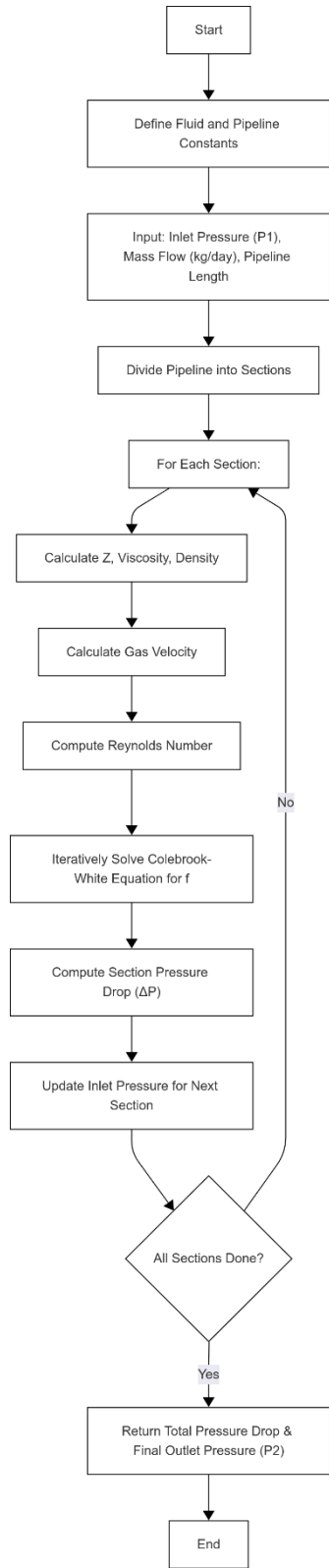


Figure 16. Flow of pressure drop calculation module

The model is tested with design mass flow rate value of 4,278,788 kg/day as mentioned in [11] and the results obtained is 26.96 bar of outlet pressure in comparison to what the study reported as 28 bar which is reasonably close approximation along with the results obtained by recreating the pressure drop plots for different ranges of mass flows for 100 mm diameter pipeline using 20 km segment length [8]. The results shown in Figure 16 imply that the pressure drop model works as intended.

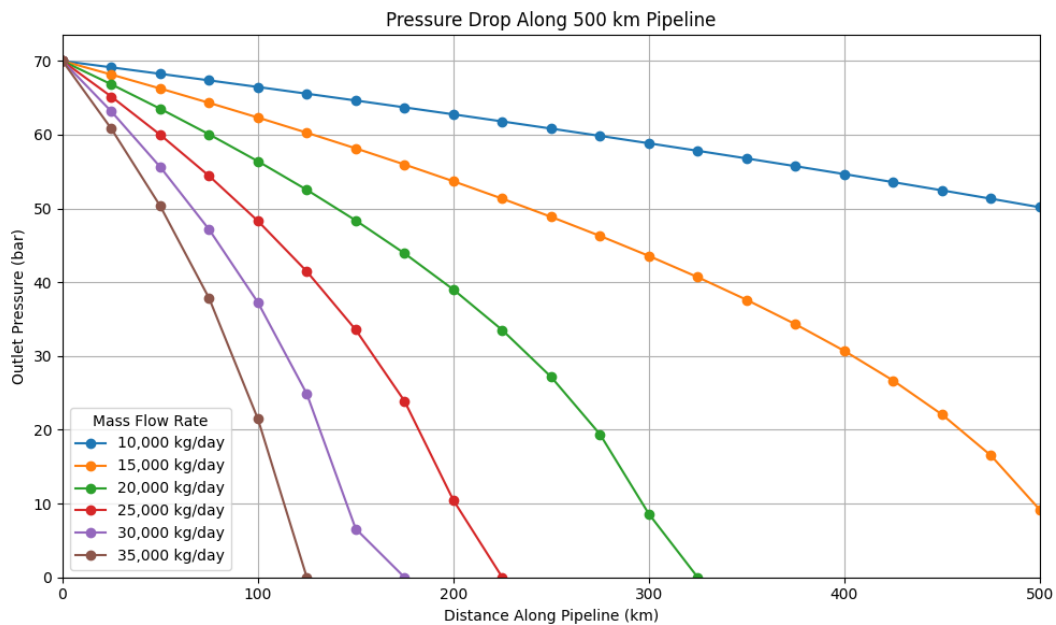


Figure 17. Pressure drops on range of mass flows for 100 mm diameter pipeline

3.3 Economical model

The last part of the model consists of economic evaluation of the pipeline. It makes use of all the equations and economic assumptions mentioned in section 1.5 and calculates the levelized cost of compression for the proposed pipeline. While the model closely follows the case study done in [11] but the difference arises as our model also includes the element of storage and thus the cost of storage becomes part of LCOH for fix speed compression case while in variable speed compression we include the cost of VFDs instead of storage.

Moreover, the energy cost comes from the calculation done by previous modules for a yearlong variable load profile with hourly resolution.

HDSAM model V5 provides us with the required relation to include geological storage site cost in the model as follows:

Installed cavern shell cost:

$$C_{cavern} = \left(2,193.5 \times \frac{V_{cav}}{9,000,000} + 7,000,000 \right) \times \frac{V_{cav}}{9,000,000} \quad (22)$$

Miscellaneous equipment installation cost:

$$C_{misc} = \left(-0.0191 \times \frac{V_{cav}}{9,000,000} + 282,603 \right) \times \frac{V_{cav}}{9,000,000} \quad (23)$$

covers piping, valves, controls and site work around the cavern.

$$C_{storage,2019USD} = C_{cavern} + C_{misc} \quad (24)$$

Because these are in 2019 USD, we need to apply CEPCI-and-FX correction to bring them into 2024 EUR:

$$C_{storage,2024EUR} = C_{storage,2019USD} \times \frac{CEPCI_{2024}}{CEPCI_{2019}} \times \frac{1}{Exchange\ rate} \quad (25)$$

Where $CEPCI_{2019}$ is taken as 619.2 [3].

While due to lack of any empirical cost relation of VFDs we have used average value of VFD as 79.93 Euro/kW based on the price of VFDs above 100kW capacity from ABB [43].

3.4 Load data and assumptions

The load data is used to realistically model the variability of gas consumption seen by compressor stations. As discussed earlier, there are four major consumers of hydrogen gas i.e Industry, power, transport and residence sector out of which industry sector is the biggest in terms of demand [5].

The data is taken from FFE open data portal. The portal provided realistic hourly hydrogen consumption data of industrial sector of Germany for the year 2025 to 2050 (though we only use first one in our simulation) [44]. The original data set is in JSON format and contains values in MW the data set is first converted to CSV using python script having pandas and json libraries.

We normalize values by dividing each data point with the maximum value to get only the behavior of the demand over time results are shown in Figure 17 and 18. This normalized profile can be used for any kind of pipeline model where the design maximum capacity is different than the consumption data

set as we will use it for our model which assumes the maximum capacity of pipeline to be 4,278,788 kg/day to ensure that we always stay within defined limits and don't run into simulation error.

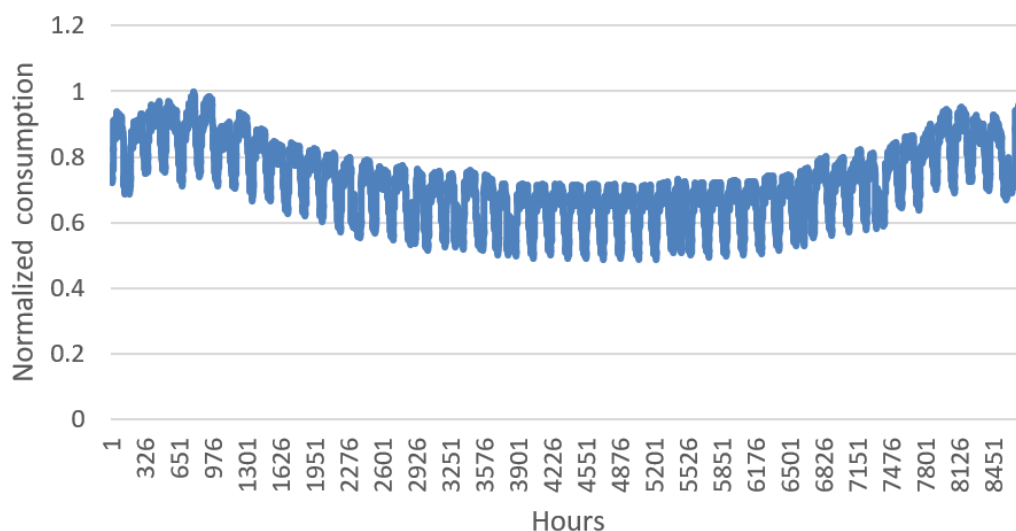


Figure 18. Predicted Hydrogen consumption pattern for Industrial sector of Germany, year 2025 [44]

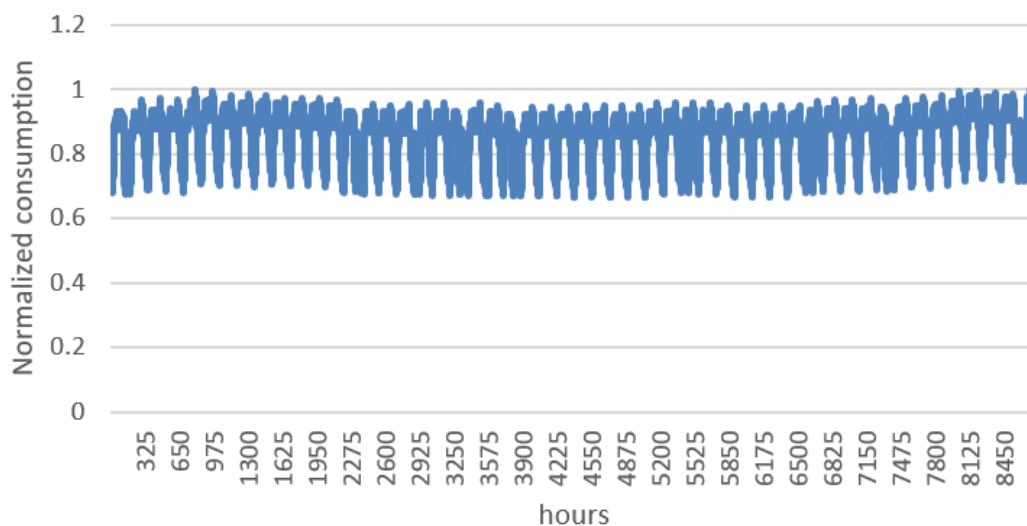


Figure 19. Predicted annual Hydrogen consumption pattern for Industrial sector of Germany, year 2050 [44]

The repeated peaks and dips seemingly show weekly variation in demand. The demand is higher on weekdays than weekends. Also there seems to be a seasonal dependency showing lower demand during the middle of the year

as compared to the ends suggesting more demand in winters than summers although the future prediction for 2050 shown in Figure 18 seems to be consistent in all seasons but still have weekdays and weekend variation.

3.5 Energy consumption comparison model

This pipeline model makes use of all the modules created above and takes the load profile as input and calculates the energy consumption in both cases i.e pipeline using fix speed compressor with storage with on/off logic for part load condition and pipeline employing variable speed compressors without storage simultaneously.

The model takes the input flow required for the hour and calculates the work done by initial compressor station. While in case when fixed speed compressors are used, we first check how many compressors can achieve this flow rate at required pressure and turn other compressors off for that moment to save energy. After that we calculate the pressure drop till the downstream enroute station and recompress the gas to maintain the required pressure i.e. 70 bar. If there is excess flow, then required as fix speed compressor can only work on design point and the excess is calculated and is stored in the storage at 200 bar along. If there is no excess, then storage compression is omitted, and flow calculation moves to the next enroute station and finally to the load. High level flow diagram of the computation is presented in Figure 19.

The loop runs for each hour and presents a summary of energy consumption in the end.

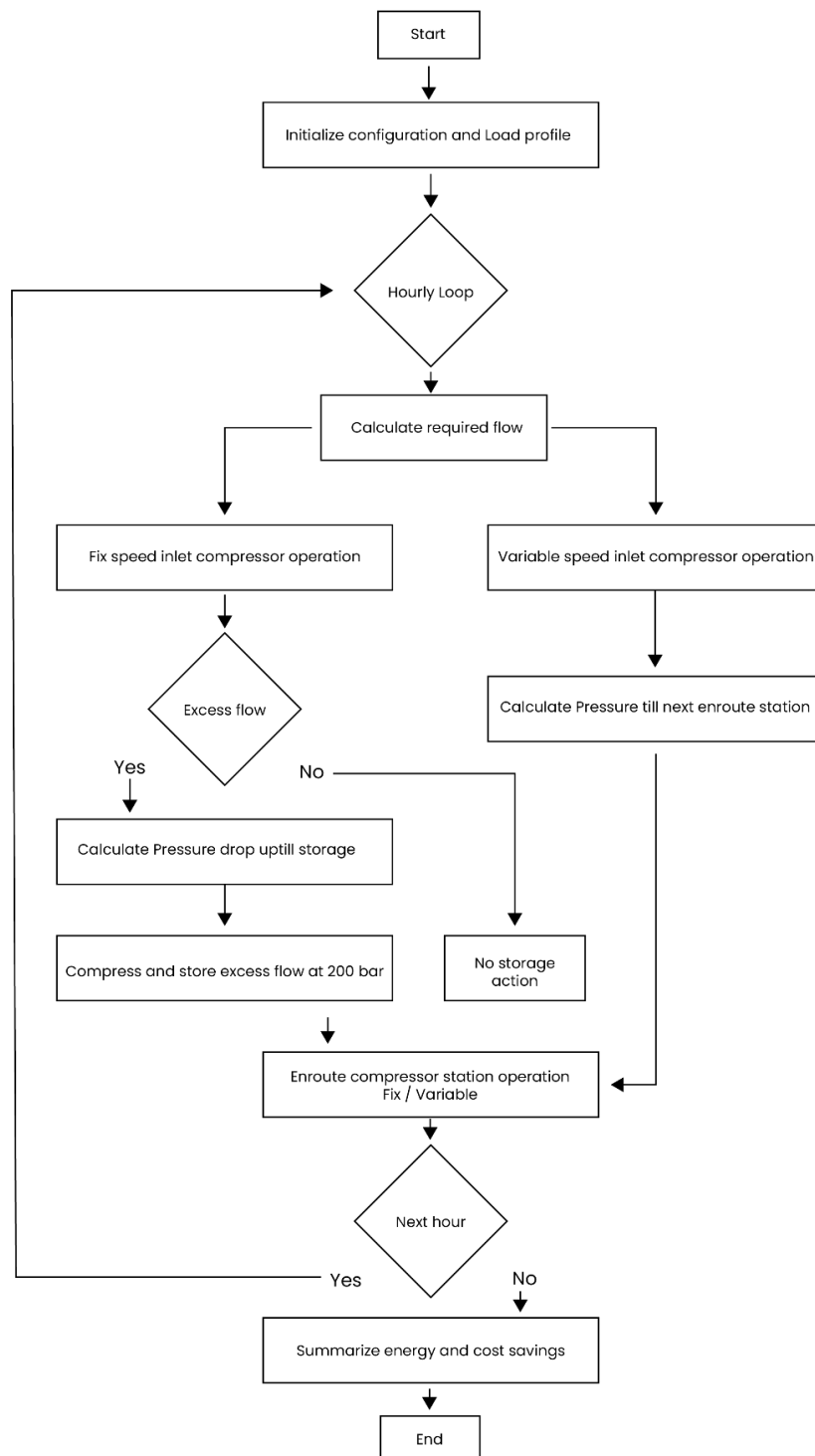


Figure 20. High level flow of energy comparison model

4 Case Study: A 1500KM Hydrogen Transmission Pipeline

The model assumes constant temperature throughout flow in a 1500km long transmission pipeline. The pipeline considered is a 36 inch steel pipe with an inlet diameter of 895.3 mm. The inlet pressure will be taken as 70 bar while outlet gas velocity at 35 m/s and compressor station will be assumed to be placed at 500km distance along pipeline while storage is placed at the middle of pipeline at 750 km as shown in Figure 20. The enroute stations will keep the pressure of the gas at desired value i.e 70 bar and compensate for any loss along the way. The inlet pressure is considered at 20 bars. Decompression for end load use is not considered.

The compressor model used for these compressor stations is centrifugal compressor having compression ratio per stage of 2.23 and isentropic efficiency of 80% and electric motor efficiency of 95% following HDSAM model developed by Argonne National Laboratory [45]p[while additionally assuming design point at 4kg/s.

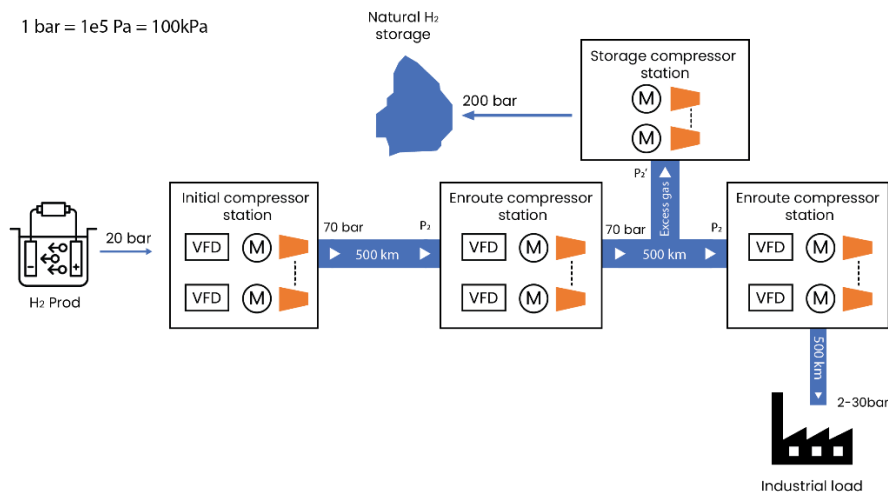


Figure 21. Hydrogen pipeline model configuration

The simulation model consists of various building blocks, including system configuration, thermodynamic calculations, compressor performance modeling, load simulation, and economic analysis. All technical parameters, e.g., suction and discharge pressures, gas constants, pipeline geometry, and compressor design specifications, are defined centrally in a configuration file.

The model is further divided into two parts, first is to calculate the energy and cost savings in both cases which is technical model while second part only calculates the economic impact by considering the cost output obtained from part 1. The model also considers the presence of sufficiently large storage; it will only be used in case of fixed speed compressor operation.

The simulation is carried out in python 3.12.2 environment with the assistance of some built in libraries such as:

- Pandas: used for reading csv data files.
- Maths: used for simple arithmetic operations
- Matplotlib: used for plotting results.
- Pyfluids: used for CoolProp to get real time values for intermediate variables like compressibility factor Z and density of Hydrogen at given temperature and pressure.
- Numpy: used for numerical functions.
- Scipy: used for interpolation.

4.1 Input parameters

Model calculations are based on the following assumptions as stated in table 4 below.

Table 4. Input parameters and assumptions for pipeline case study model

Factor	Value	Notes/Reference
Suction pressure of inlet compressor (bar)	20	Initial pressure after production, typical from SMR H ₂ plant
Discharge pressure of inlet compressor (bar)	70 - 100	= inlet pressure of pipeline
Suction Temperature (T_{suc})	293.15	[3]
Isentropic efficiency % (η_{isen})	75	Based on performance map used for modeling. Design point efficiency.
Compression ratio per stage (x)	2.23	[11], used for getting desired output pressure of 70 or 100 bar

Maximum compressor size (kW)	16,000	[11]
Design point mass flow output (kg/s)	4	Based on performance map used for modeling.
H2 viscosity (kg/m.s)	0.0000087	[46]
H2 gas gravity	0.0696	[47]
Elevation difference (m)	100	[11]
Flow temperature (K)	288.15	[11]
Base pressure (bar)	1.01	= 101 kPa
Base Temperature (K)	288.71	[48]
Pipe roughness (mm)	0.0178	[49]
Outlet gas velocity (m/s)	35	[11]
Pipe Length (km)	500	[11], distance between each downstream compressor station
Total distance (km)	1,500	[11]
Segment length (km)	20	[8], Used in pressure drop calculation.
Maximum capacity, pipeline (kgH2/day)	4,278,788	[11]
Specific gas constant (J/kg.K)	4124	[50]
Motor efficiency % (η_{motor})	95	[11]
Storage distance (km)	750	= $\frac{\text{Total distance}}{2}$ in between the downstream compressor stations.
Storage capacity (million m³)	100	
VFD efficiency (%)	98.5	[18]

4.2 Test 24-hour variable load profile

First, we have tested the model integrity by using a pseudo 24 hour variable load profile that ranges between 50 to 100 percent full load. In table 5 below, we can see that the number of working compressor units are changing based on required flow rate that was the desired outcome to save energy as much as possible while for storage station we only need one unit to always meet the required mass flow requirement. From the table we can also see that the

pressure drop at enroute stations increases with the increase of mass flow rate as discussed in section 3.2 earlier.

Table 5. Model technical computational results

Hour (h)	Load Fraction	Flow (kg/s)	Working compressor units	Inlet pressure at enroute stations (bar)	Excess flow (kg/s)	Pressure at storage inlet (bar)
0	0.5	24.74	7	61.39	3.26	64.89
1	0.51	25.16	7	61.09	2.84	64.89
2	0.53	26.4	7	60.17	1.6	64.89
3	0.57	28.36	8	58.6	3.64	63.33
4	0.62	30.92	8	56.32	1.08	63.33
5	0.69	33.91	9	53.32	2.09	61.53
6	0.75	37.11	10	49.6	2.89	59.49
7	0.81	40.31	11	45.26	3.69	57.17
8	0.88	43.29	11	40.51	0.71	57.17
9	0.93	45.85	12	35.69	2.15	54.54
10	0.97	47.82	12	31.36	0.18	54.54
11	0.99	49.05	13	28.24	2.95	51.57
12	1	49.48	13	27.09	2.52	51.57
13	0.99	49.05	13	28.24	2.95	51.57
14	0.97	47.82	12	31.36	0.18	54.54
15	0.93	45.85	12	35.69	2.15	54.54
16	0.88	43.29	11	40.51	0.71	57.17
17	0.81	40.31	11	45.26	3.69	57.17
18	0.75	37.11	10	49.6	2.89	59.49
19	0.69	33.91	9	53.32	2.09	61.53
20	0.63	30.92	8	56.32	1.08	63.33
21	0.57	28.36	8	58.6	3.64	63.33
22	0.53	26.4	7	60.17	1.6	64.89
23	0.51	25.16	7	61.09	2.84	64.89

Apart from the technical calculations we also compute the energy consumed at each stage of the model as given in Table 6.

Table 6. Model Energy computation results

Hour (h)	Storage Station Energy Consumption (kWh)	Stored H ₂ (kg)	Initial Station Energy Consumption (kWh)		Enroute Stations Energy Consumption (kWh)	
			Fix	Variable	Fix	Variable
			0	6723.99	11743.39	64835.22
1	5855.24	21969.52	64835.22	49289.64	13001.15	10129.27
2	3308.19	27747.25	64835.22	53701.85	14461.57	12268.94
3	7677.28	40848.6	74097.39	54965.02	19457.71	14770.01
4	2273.2	44727.84	74097.39	64252.05	23857.19	21140.69
5	4538.27	52267.7	83359.56	68931.18	33739.21	28459.81
6	6464.83	62682.78	92621.74	74523.02	47687.68	39053.21
7	8545.38	75973.1	101883.9	80168.24	66829.93	53384.63
8	1640.2	78524.03	101883.9	91624.98	84514.59	76940.66
9	5173.97	86252.85	111146.1	94308.26	114584.4	98140.49
10	436.77	86905.3	111146.1	102561.6	137892.8	128108
11	7435.24	97509.34	120408.3	99861.23	170122.3	141787.8
12	6371.38	106596.1	120408.3	101425.6	178448.4	150953.5
13	7435.24	117200.2	120408.3	99861.23	170122.3	141787.8
14	436.77	117852.6	111146.1	102561.6	137892.8	128108
15	5173.97	125581.4	111146.1	94308.26	114584.4	98140.49
16	1640.2	128132.4	101883.9	91624.98	84514.59	76940.66
17	8545.38	141422.7	101883.9	80168.24	66829.93	53384.63
18	6464.83	151837.8	92621.74	74523.02	47687.68	39053.21
19	4538.27	159377.6	83359.56	68931.18	33739.21	28459.81
20	2273.2	163256.9	74097.39	64252.05	23857.19	21140.69
21	7677.28	176358.2	74097.39	54965.02	19457.71	14770.01
22	3308.19	182136	64835.22	53701.85	14461.57	12268.94
23	5855.24	192362.1	64835.22	49289.64	13001.15	10129.27

Based on tables 5 and 6 we can create a chart comparing energy savings percentage for each hour as shown in Figure 21 that the model correctly computes the energy savings for each hour. The trend suggests that the variable speed drive is relatively more useful for partial load conditions and saves more energy at lower loads but still saves up to minimum of 8% at 97% flow rate of 47.82 kg/s condition. The difference of energy consumption in fix and variable speed computations at varying load comes from the fact that fix speed compressor setup always works at design point using $13 \times 4 = 52 \text{ kg/s}$ mass flow while variable speed is using instantaneous mass flow and lower rpm thus resulting in lower energy consumption. Since even at 100% flow rate the maximum flow is still less than design flow, the VSDs still consume less energy.

The overall percentage saving is calculated to be 18% for this load profile savings us an energy cost of 134,895 Euro/day using 0.1867 euro/kWh tariff. Another noticeable thing is the random behavior of percentage savings from VSDs. Apparently, the compressors turning on and off are the cause of the erratic fluctuations in hourly savings. Fixed-speed energy jumps by a machine's full load when demand reaches a threshold, but variable-speed energy jumps in a different way, resulting in a leap in the percentage of savings. Near design flow both run near peak efficiency, so the gap narrows. At low flow, the VFD throttles speed ($\text{power} \propto n^3$) to cut energy much more than fixed speed, so savings appear enormous. Additionally, the ratio is skewed by the additional kwh if we only use storage compression in fixed speed case.

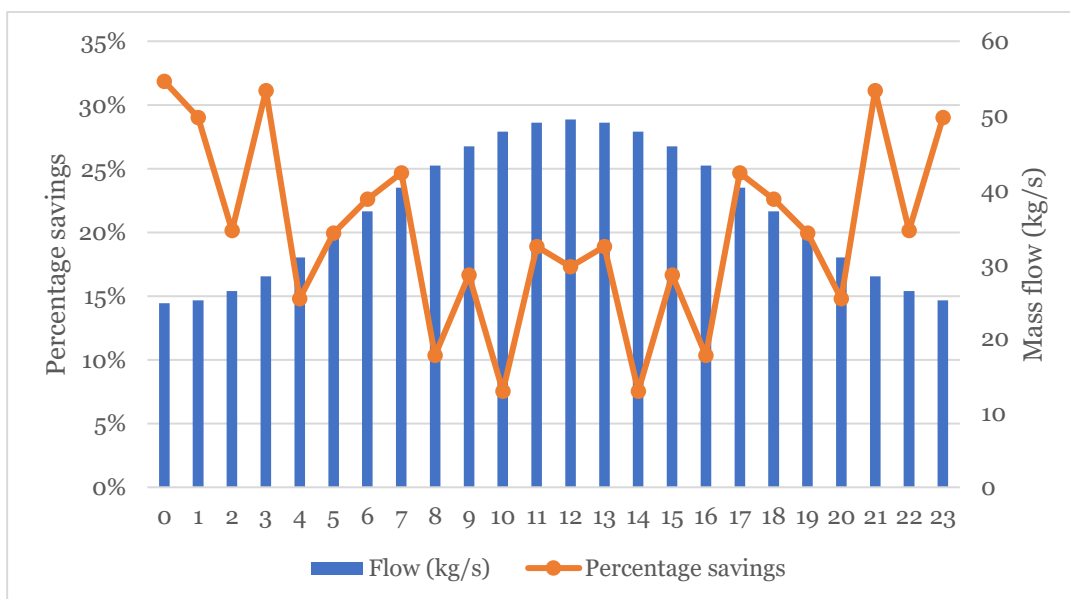


Figure 22. Hourly energy savings vs mass flow

4.3 Energy consumption comparison for variable Industrial load

After verifying the model, we input a yearlong industrial hydrogen load profile to the model. The aim is to compare the compression energy consumption in each scenario i.e. fix and variable speed. The simulation is run for two pipeline pressure levels i.e. 70 bar and 100 bar. The results are presented in table 7.

Table 7. Compression energy consumption comparison for 70 and 100 bar pipeline pressure

Metric	Pipeline pressure (70 bar)		Pipeline pressure (100 bar)	
	Fix speed op	Variable speed op	Fix speed op	Variable speed op
Energy consumption (kWh)				
Initial Station	784,940,400.49	644,601,087.04	1,042,899,479.51	856,439,721.73
Enroute Stations	418,390,001.43	345,901,946.14	169,895,399.81	140,278,510.45
Storage station	35,038,028.14	-	25,324,728.22	-
Total	1,203,330,401.9	990,503,033.19	1,238,119,607.54	996,718,232.17
Savings				
Percentage energy (%)	-	20.4	-	19.5
Cost savings (Euro/year)	-	47,261,077	-	45,069,637
Energy Intensity (kWh/kg)				
Initial station	0.701	0.575	0.931	0.764
Enroute station	0.373	0.309	0.152	0.125

From the table we can see that the results are following the theory of energy saving when using variable speed compressors in part load conditions. One thing to notice is that the energy consumption of enroute, storage and initial stations depend significantly on the initial pressure of pipeline. For the case of 70 bar pipeline pressure, we see that initial stations consume less energy

as compared to the 100 bar pipeline pressure case. That is because the initial stations are working more to raise the pressure level in later cases as compared to the former.

While the results are opposite in enroute and storage compression stations as discussed before in section 3.2 the pressure drop is lower if initial pressure is higher as a result when initial stations raise the pressure to 100 bar in the start, all the downstream stations see lesser pressure drops as compared to 70 bar case as a result they consume less energy to maintain the pressure of pipeline or to store hydrogen in the geological storage.

4.4 LCOH results

The levelized cost of hydrogen compression is calculated using the equations presented in section 2.5 and energy consumption values presented in table 7 in the previous section. The currency value is converted according to 2024 Euro exchange rate presented in section 2.4.

Table 8. Levelized cost of compression results for 70 and 100 bar pipeline pressure cases

Metric	Fix Total 70 bar	Var Total 70 bar	Fix Total 100 bar	Var Total 100 bar
CAPEX (€ Million)	206.94	224.6	206.94	224.6
Electricity (€ Million)	231.2	134.81	230.71	135.66
Labor (€ Million)	4.65	4.65	4.65	4.65
O&M (€ Million)	87.81	95.3	87.81	95.3
CAPEX (per kg)	0.13	0.12	0.13	0.12
Non energy OPEX / Labor + O&M (per kg)	0.06	0.06	0.06	0.06
Energy OPEX (per kg)	0.20	0.16	0.20	0.16
LCOH (per kg)	0.39	0.35	0.39	0.35

Table 8 shows us that whether the pipeline pressure is 70 bar or 100 bar, it does not have a significant effect on overall cost in the end as CAPEX and non-energy OPEX remain the same in both cases while only changing factor is energy OPEX which also comes out to be almost equal.

4.5 Sensitivity of changing maximum flow rate

We also look at the economic results by changing the maximum flow rate and required number of compressors. We use four scenarios to see the effect on overall cost of compression in proposed pipelines.

- 1- Using 40% design capacity as max capacity i.e. $4,278,788 * 0.4 = 1,711,515.2$ kg/day = 19.8 kg/s that requires 5 compressors at initial and enroute stations.
- 2- Using 60% of design capacity as max capacity i.e. $4,278,788 * 0.6 = 2,567,272.8$ kg/day = 29.7 kg/s that requires 8 compressors at initial and enroute stations.
- 3- Using 80% of design capacity as max capacity i.e. $4,278,788 * 0.8 = 3,423,030.4$ kg/day = 39.6 kg/s that requires 10 compressors at initial and enroute stations.
- 4- Original design capacity of 4,278,788 kg/day equal to 49.52 kg/s requiring 13 of compressors at each station.

The number of maximum compressors at storage station was calculated dynamically in the model. That means in the economic cost calculation for fixed speed pipeline we must account for the extra compressor station having extra compressors for storing hydrogen as well.

Table 9. LCOH vs maximum flow capacity

Scenario	Mode	CAPEX €/kg	Energy OPEX €/kg	Non-energy OPEX €/kg	LCOH €/kg
40% of capacity	Fixed	0.16	0.16	0.07	0.39
40% of capacity	Variable	0.13	0.11	0.06	0.30
60% of capacity	Fixed	0.15	0.16	0.07	0.38
60% of capacity	Variable	0.14	0.12	0.06	0.32
80% of capacity	Fixed	0.13	0.17	0.06	0.36
80% of capacity	Variable	0.13	0.13	0.06	0.32
100% capacity	Fixed	0.13	0.20	0.06	0.39
100% capacity	Variable	0.12	0.16	0.06	0.35

The capital cost needed to construct and install the pipeline and compressor infrastructure is shown in the "CAPEX €/kg" column and is divided by the total amount of hydrogen transported. Because less hydrogen is transported using the same infrastructure at lower flows, this cost per kilogram rises. The cost of electricity used by the compressors is shown in the "Energy OPEX €/kg" column.

Variable-speed systems scale their energy use with demand, resulting in lower energy costs per kilogram at reduced flows, whereas fixed-speed systems consume almost constant power regardless of flow, making them less efficient at lower capacities. Operational costs unrelated to energy, like labor, maintenance, and insurance, are included in the "Non-energy OPEX €/kg." At lower flow rates, these become more significant on a per-kilogram basis and are comparatively fixed.

As anticipated, the underutilization of fixed capital and operational infrastructure was the main cause of the LCOH's increase as flow declined. The LCOH was 0.39 €/kg for fixed-speed compressors and 0.35 €/kg for variable-speed compressors operating at 100% design capacity. The LCOH rose to 0.39 €/kg (fixed) and 0.30 €/kg (variable) when running at only 40% capacity, demonstrating the benefit of load-following compressor strategies.

Because the total capital investment stays constant while the amount of hydrogen transported falls, it is noteworthy that CAPEX per kg hydrogen increases at lower flow rates. For instance, in the fixed speed scenario, CAPEX went from 0.13 €/kg at 100% capacity to 0.16 €/kg at 40%. On the other hand, due to their more adaptable operation, the variable speed system maintained a more stable CAPEX per kg, exhibiting only a minor increase from 0.12 €/kg to 0.13 €/kg over the whole flow range.

Additionally, there was flow dependence on energy-related operating costs (Energy OPEX). The inefficiencies of running fixed-speed compressors at partial load were reflected in Energy OPEX, which varied from 0.16 €/kg at 40% to 0.20 €/kg at 100%. Conversely, variable-speed compressors continued to operate more efficiently at lower flow rates, with Energy OPEX increasing more subtly from 0.11 €/kg to 0.16 €/kg during the same range.

Variable-speed compressors continuously performed better than fixed-speed systems in terms of overall cost and energy efficiency across all scenarios. The LCOH difference between fixed-speed and variable-speed systems peaked at 40% flow (0.30 €/kg vs. 0.39 €/kg), highlighting the significance

of adaptable compressor operation in underloaded systems. The LCOH difference decreases as flow gets closer to design capacity, with both modes convergent toward 0.35 - 0.39 €/kg.

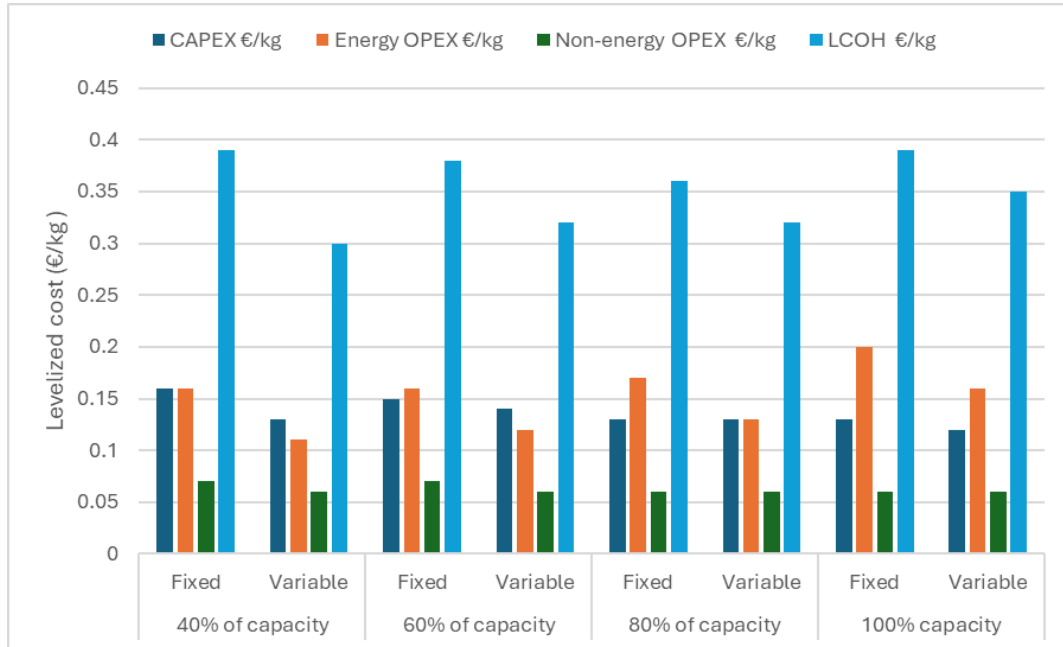


Figure 23. LCOH vs maximum flow capacity chart

Looking at table 9 and Figure 22. It shows us that the economics are severely penalized when the pipeline is operated below its design capacity, especially for fixed-speed systems. By increasing part-load efficiency and maximizing installed capacity, variable-speed operation reduces these losses and is therefore a more economical option in a range of flow conditions.

4.6 Sensitivity of changing number of enroute stations and spread distance

Next, we simulate 4 scenarios with different numbers of enroute stations and their placement along the total length of pipeline.

The scenarios are as follows:

- 1- Assuming 5 enroute stations placed at distance of 250 km each
- 2- Assuming 4 enroute stations placed at distance of 300 km each
- 3- Assuming 3 enroute stations placed at distance of 375 km each
- 4- Assuming 2 enroute stations placed at distance of 500 km each

The maximum flow rate is the same for all scenarios i.e. 4,278,788 kg/day along with the number of compressor units i.e. 13 for each station except storage which is calculated dynamically to be just 1 as excess flow is always less than the design capacity of one compressor i.e. 4kg/s.

Table 10. LCOH vs. En-Route Station Count

Scenario	Mode	CAPEX €/kg	Energy OPEX €/kg	Non-energy OPEX €/kg	LCOH €/kg
5 enroute stations	Fixed	0.23	0.20	0.11	0.54
	Variable	0.26	0.16	0.12	0.54
4 enroute stations	Fixed	0.20	0.20	0.09	0.49
	Variable	0.22	0.16	0.10	0.48
3 enroute stations	Fixed	0.16	0.20	0.07	0.43
	Variable	0.18	0.16	0.08	0.42
2 enroute stations	Fixed	0.13	0.20	0.06	0.39
	Variable	0.13	0.16	0.06	0.35

From table 10 and figure 23 we can see that increasing the number of stations lead to higher capital cost per kilogram of hydrogen. This happens due to the proportional increase in equipment installed and its cost. For example, fixed speed CAPEX rose 0.13 €/kg for the 2-station configuration to 0.23 €/kg with 5 station and a similar trend is observed for variable speed configuration as well. Non energy OPEX which mainly includes the labor and maintenance also increases with station count reflecting the large asset base. Interestingly the energy related operational cost while seemingly constant at 0.2 and 0.16 €/kg for fixed and variable speed cases but the raw energy consumption values in Table 11 suggest there still is variation in total energy consumption with each configuration but its relatively small to make a big difference in normalized value. Nonetheless the energy savings in variable speed configuration are unavoidable.

Furthermore, the results suggest that the overall LCOH benefits of variable speed configuration are dominant in the base case of 2 enroute stations and it decreases as we increase the station count due to additional investment and maintenance cost.

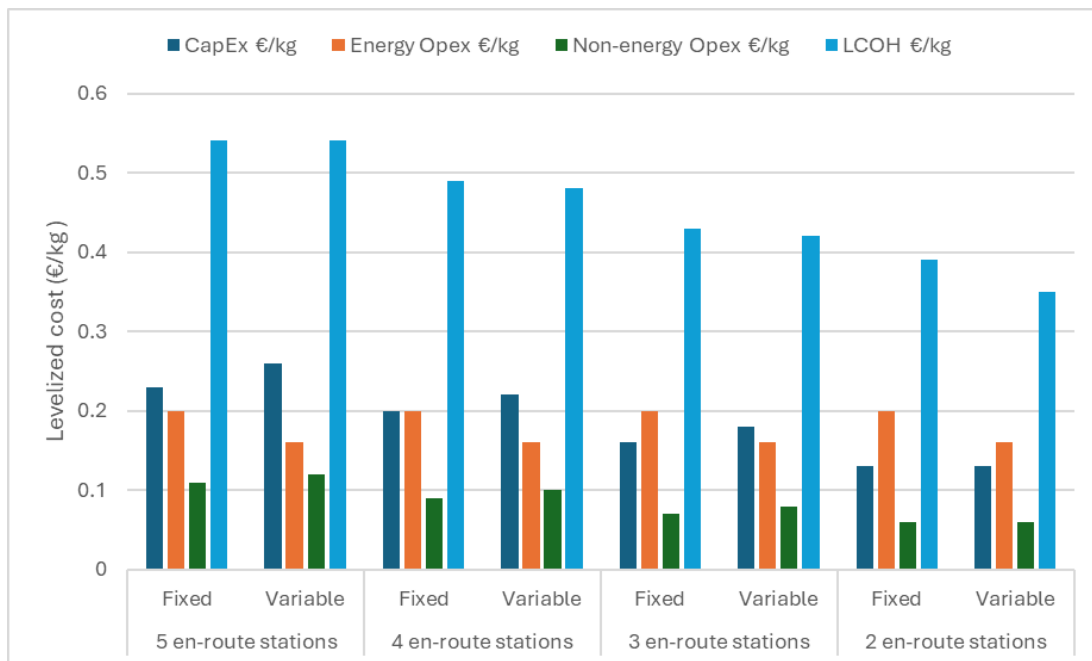


Figure 24. LCOH vs. En-Route station count chart

Table 11 also shows us how initial station energy consumption stays constant in each configuration as the flow and pipeline pressure is constant i.e. 4,278,788 kg/day at 70 bar respectively. One interesting thing to notice is the non-monotonic nature of the trend for example the energy consumption for enroute compressor stations for 2 enroute stations is 414,161 MWh and it decreases for 3 stations as we can imagine that by increasing the station we decrease the segment length that gas has to travel thus lower pressure drop and lower work done by enroute compressors but it again increases for 4 enroute station even though now the segment length is 300 km as compared to 375 km before.

The discrepancy is due to the increased number of operating compressors and increase in associated energy losses which outweigh the benefit of lower travel distance for gas. This behaviour seems closer to the real world and consistent with established gas pipeline engineering principles [51]. Also supported by study suggesting that adding booster stations doesn't always improve energy efficiency but there is an optimal spacing requirement needed to get the best results. [52]

Table 11. Energy consumption at each station

Scenario	Initial Station (MWh)		Enroute Stations (MWh)	
	Fixed	Variable	Fixed	Variable
5 enroute stations	762490	627701	393535	325672
4 enroute stations	762490	627701	411243	340399
3 enroute stations	762490	627701	388551	321697
2 enroute stations	762490	627701	414161	343186

Results obtained from our model suggest the best energy OPEX is obtained in the case of 3 enroute stations but the best overall results are obtained in the case of 2 enroute stations.

5 Conclusion

The thesis presents a comprehensive techno economic comparison of two hydrogen pipelines compression strategies i.e. fixed speed compressor along with storage versus variable speed compressors without storage by integrating real gas pipeline hydraulics empirical compressor performance map and economic evaluation framework. A centrifugal compressor map was interpolated using SciPy's LinearNDinterpolator to predict rotational speed and isentropic efficiency dynamically enabling an accurate estimation of energy consumption requirement across a yearlong varying load profile with hourly resolution. Geological storage storing the excess hydrogen gas at 200bar was also included in fixed speed compression strategy while for simplicity, only the compression of excess gas was considered without considering the control strategy to sue the stored hydrogen for demand management.

The modular simulation framework was designed to facilitate flexible scenario analysis and validated against known cases. The findings demonstrated that by dynamically modifying shaft speed and utilizing affinity laws, variable-speed drives (VSDs) continuously decreased compressor energy consumption by 18% in a 24-hour test and by up to 20.4% over an industrial demand profile. Across all tested pressure and flow scenarios, the levelized cost of hydrogen (LCOH) was reduced by roughly 0.06 €/kg, or 15 - 20%, due to electricity savings, even though VSDs had slightly higher capital costs. Notably, LCOH for VSDs was further decreased when operating at lower flow rates, demonstrating the advantages of strategic flow modulation.

These findings were further supported by sensitivity analyses. Fixed-speed systems experienced disproportionately higher LCOH values when the pipeline was operated below its design capacity, while variable-speed compressors maintained their economic performance and efficiency, highlighting their versatility. Similarly, a non-linear relationship between energy consumption and station count was found when the number and location of enroute stations were changed. Although more stations lower segment pressure drops, the advantages are eventually outweighed by the additional energy overhead and maintenance expenses. While at the same time, even though fewer enroute compressor stations lower the CAPEX and non-energy OPEX but optimal spacing is required as with 2 compressor stations placed 500 km apart the flow drops to as low as 27 bar required for distribution purpose [53]. These findings are consistent with well-established engineering literature that identifies the ideal compression station spacing to reduce the total energy demand of the system.

Finally, under variable-load conditions, variable-speed compression is the best approach for hydrogen transport pipelines. It offers faster payback on VFD investments, drastically lowers operating energy, and does away with the need for large-scale buffer storage. Future developments of the model might incorporate a strong storage utilization control strategy, employ sophisticated compressor maps based on realistic 80% isentropic efficiencies, and take decompression at downstream distribution points into consideration in order to better match the simulation with actual hydrogen infrastructure.

References

- [1] A. O. Oni, K. Anaya, T. Giwa, G. Di Lullo, and A. Kumar, “Comparative assessment of blue hydrogen from steam methane reforming, autothermal reforming, and natural gas decomposition technologies for natural gas-producing regions,” *Energy Convers. Manag.*, vol. 254, p. 115245, Feb. 2022, doi: 10.1016/j.enconman.2022.115245.
- [2] “Throttling Loss - an overview | ScienceDirect Topics.” Accessed: May 14, 2025. [Online]. Available: <https://www.sciencedirect.com/topics/engineering/throttling-loss>
- [3] M. A. Khan, C. Young, and D. B. Layzell, “The Techno-Economics of Hydrogen Pipelines,” vol. 1, no. 2, 2021.
- [4] G. Molnar, “Economics of Gas Transportation by Pipeline and LNG,” in *The Palgrave Handbook of International Energy Economics*, M. Hafner and G. Luciani, Eds., Cham: Springer International Publishing, 2022, pp. 23–57. doi: 10.1007/978-3-030-86884-0_2.
- [5] “EHB-Analysing-the-future-demand-supply-and-transport-of-hydrogen-June-2021-v3.”
- [6] I. A. Gondal, “Hydrogen transportation by pipelines,” in *Compendium of Hydrogen Energy*, Elsevier, 2016, pp. 301–322. doi: 10.1016/B978-1-78242-362-1.00012-2.
- [7] “Density of Elements Chart – Angstrom Sciences Elements Density Table,” angstromsciences. Accessed: May 22, 2025. [Online]. Available: <https://angstromsciences.com/density-elements-chart>
- [8] Mithran Daniel Solomon, W. Heineken, M. Scheffler, and T. Birth, “PRESSURE DROP IN PIPELINES TRANSPORTING COMPRESSED HYDROGEN GAS,” Fraunhofer Institute for Factory Operation and Automation, Energy Systems and Infrastructures, Energy and Resource Efficient Systems, 2023.
- [9] C. Hora, F. C. Dan, D.-C. Secui, and H. N. Hora, “Systematic Literature Review on Pipeline Transport Losses of Hydrogen, Methane, and Their Mixture, Hythane,” *Energies*, vol. 17, no. 18, Art. no. 18, Jan. 2024, doi: 10.3390/en17184709.
- [10] V. Lemort and A. Legros, “Positive displacement expanders for Organic Rankine Cycle systems,” in *Organic Rankine Cycle (ORC) Power Systems*, Elsevier, 2017, pp. 361–396. doi: 10.1016/B978-0-08-100510-1.00012-0.
- [11] M. A. Khan, C. Young, C. MacKinnon, and D. B. Layzell, “The Techno-Economics of Hydrogen Compression,” vol. 1, no. 1, 2021.
- [12] “Centrifugal compressor,” Jan. 2025, doi: 10.2118/PW0113.
- [13] S.-A. Kim and K.-P. Hong, “Analysis and Experimental Verification of a Variable Speed Turbo Air Centrifugal Compressor System for Energy Saving,” *Energies*, vol. 14, no. 4, p. 1208, Feb. 2021, doi: 10.3390/en14041208.
- [14] C. Ocak, M. Koşan, S. Erten, F. Nur Erdoğan, and M. Öder, “Comparison of different compressor technologies for refrigerated display

- cabinet: Experimental study,” *Mater. Today Proc.*, vol. 81, pp. 74–80, 2023, doi: 10.1016/j.matpr.2023.01.213.
- [15] R. S. Adhikari, N. Aste, M. Manfren, and D. Marini, “Energy Savings through Variable Speed Compressor Heat Pump Systems,” *Energy Procedia*, vol. 14, pp. 1337–1342, 2012, doi: 10.1016/j.egypro.2011.12.1098.
- [16] J. Tolvanen, “Saving energy with variable speed drives,” *World Pumps*, vol. 2008, no. 501, pp. 32–33, Jun. 2008, doi: 10.1016/S0262-1762(08)70164-0.
- [17] X. Guo, X. Hu, and S. Zhang, “Application status of variable-frequency drive in hydrogen fuel cell air compressors from an industrial viewpoint: A review,” *Sustain. Energy Technol. Assess.*, vol. 64, p. 103716, Apr. 2024, doi: 10.1016/j.seta.2024.103716.
- [18] “ACS5000 technical data,” Drives. Accessed: May 13, 2025. [Online]. Available: <https://new.abb.com/drives/medium-voltage-ac-drives/acs5000/acs5000-technical-data>
- [19] “SINAMICS G120X infrastructure pump, fan & compressor drive,” Siemens USA. Accessed: May 06, 2025. [Online]. Available: <https://www.siemens.com/us/en/products/drives/sinamics-electric-drives/low-voltage-drives/standard-performance-drives/sinamics-g120x.html>
- [20] “SINAMICS S120,” siemens.com Global Website. Accessed: May 13, 2025. [Online]. Available: <https://www.siemens.com/global/en/products/drives/sinamics/low-voltage-converters/servo-converter/sinamics-s120.html>
- [21] “VLT® AutomationDrive FC 301 / FC 302.” Accessed: May 06, 2025. [Online]. Available: <https://www.danfoss.com/en-us/products/dds/low-voltage-drives/vlt-drives/vlt-automationdrive-fc-301-fc-302/>
- [22] “PowerFlex 755 AC Drives | Allen-Bradley | US,” Rockwell Automation. Accessed: May 06, 2025. [Online]. Available: <https://www.rockwellautomation.com/en-us/products/hardware/allen-bradley/vfd/low-voltage-ac-drive/architecture-drive/20g-powerflex-755.html>
- [23] R. Automation, “PowerFlex 750-Series Products with TotalFORCE Control Technical Data”.
- [24] “A1000 Drive - Yaskawa.” Accessed: May 06, 2025. [Online]. Available: <https://www.yaskawa.com>
- [25] “Altivar Process 630 Variable Frequency Drives VFD | Schneider Electric USA.” Accessed: May 06, 2025. [Online]. Available: <https://www.se.com/us/en/product-range/62317-altivar-process-630-variable-frequency-drives-vfd/>
- [26] “ATV930D75N4C - variable speed drive, Altivar Process ATV900, ATV930, 75kW, 400 to 480V, without braking unit, IP21 | Schneider Electric Egypt.” Accessed: May 13, 2025. [Online]. Available: <https://www.se.com/eg/en/product/ATV930D75N4C/variable-speed-drive-altivar-process-atv900-atv930-75kw-400-to-480v-without-braking-unit-ip21/>

- [27] “Mitsubishi Electric Factory Automation - EMEA.” Accessed: May 06, 2025. [Online]. Available: <https://emea.mitsubishielectric.com/fa>
- [28] “FRENIC-MEGA Inverter Drive,” Fuji Electric Corp. of America. Accessed: May 06, 2025. [Online]. Available: <https://americas.fujielectric.com/products/vfd-inverters-ac-drives/frenic-mega/>
- [29] “EU hourly labour costs ranged from €11 to €55 in 2024.” Accessed: May 07, 2025. [Online]. Available: <https://ec.europa.eu/eurostat/web/products-eurostat-news/w/ddn-20250328-1>
- [30] “Yearly average currency exchange rates | Internal Revenue Service.” Accessed: May 11, 2025. [Online]. Available: <https://www.irs.gov/individuals/international-taxpayers/yearly-average-currency-exchange-rates>
- [31] “Cost Indices – Towering Skills.” Accessed: May 11, 2025. [Online]. Available: https://toweringskills.com/financial-analysis/cost-indices/?utm_source=chatgpt.com
- [32] Y. Li, “Hydrogen Sourced from Renewables and Clean Energy: A Feasibility Study of Achieving Large-scale Demonstration”.
- [33] “Electricity price statistics.” Accessed: May 11, 2025. [Online]. Available: https://ec.europa.eu/eurostat/statistics-explained/index.php?title=Electricity_price_statistics
- [34] “EU hourly labour costs ranged from €11 to €55 in 2024.” Accessed: May 11, 2025. [Online]. Available: <https://ec.europa.eu/eurostat/web/products-eurostat-news/w/ddn-20250328-1>
- [35] “Review of Hydrogen Storage Technologies and the Crucial Role of Environmentally Friendly Carriers | Energy & Fuels.” Accessed: May 06, 2025. [Online]. Available: https://pubs.acs.org/doi/10.1021/acs.energyfuels.4c01781?utm_source=chatgpt.com
- [36] M. M. Rampai, C. B. Mtshali, N. S. Seroka, and L. Khotseng, “Hydrogen production, storage, and transportation: recent advances,” *RSC Adv.*, vol. 14, no. 10, pp. 6699–6718, doi: 10.1039/d3ra08305e.
- [37] W. Fang *et al.*, “Review of Hydrogen Storage Technologies and the Crucial Role of Environmentally Friendly Carriers,” *Energy Fuels*, vol. 38, no. 15, pp. 13539–13564, Aug. 2024, doi: 10.1021/acs.energyfuels.4c01781.
- [38] M. N. Sarker, A. N. Sakib, M. I. H. Al-Mobin, and P. M. Resnick, “Innovative Materials and Techniques for Enhancing Hydrogen Storage: A Comprehensive Review of Damage Detection and Preventive Strategies,” *ASME Open J. Eng.*, vol. 3, no. 031011, May 2024, doi: 10.1115/1.4065360.
- [39] C. Yang *et al.*, “Demands and challenges of large-scale salt cavern hydrogen storage in China,” *Rock Soil Mech.*, vol. 45, no. 1, pp. 1–19, Jan. 2024, doi: 10.16285/j.rsm.2023.6785.
- [40] A. Ebrahimi, K. Ghasemi, A. Akbari, Y. Kazemzadeh, and R. Azin, “Hydrogen Energy System and Underground Hydrogen Storage in Depleted Reservoirs,” *Pet. Res.*, Apr. 2025, doi: 10.1016/j.ptlrs.2025.04.002.

- [41] E. I. Epelle *et al.*, “Perspectives and prospects of underground hydrogen storage and natural hydrogen,” *Sustain. Energy Fuels*, vol. 6, no. 14, pp. 3324–3343, 2022, doi: 10.1039/D2SE00618A.
- [42] “LinearNDInterpolator — SciPy v1.15.3 Manual.” Accessed: May 13, 2025. [Online]. Available: <https://docs.scipy.org/doc/scipy/reference/generated/scipy.interpolate.LinearNDInterpolator.html>
- [43] “ABB Variable Frequency Drives Price List.” Accessed: May 12, 2025. [Online]. Available: <http://www.vfds.org/abb-vfd-price-list-346980.html>
- [44] “Load Curves of the Industry Sector including Feedstock (Europe NUTS-3) – opendata.ffe.de.” Accessed: May 12, 2025. [Online]. Available: <https://opendata.ffe.de/dataset/load-curves-of-the-industry-sector-including-feedstock-europe-nuts-3/>
- [45] Amgad Elgowainy, K. Reddi, M. Mintz, and D. Brown, “Hydrogen Delivery Infrastructure Analysis,” Argonne National Laboratory, 2013.
- [46] “Gas Reference | CONCOA.” Accessed: May 13, 2025. [Online]. Available: https://www.concoa.com/gas_reference#Hydrogen
- [47] “Gases - Specific Gravities.” Accessed: May 13, 2025. [Online]. Available: https://www.engineeringtoolbox.com/specific-gravities-gases-d_334.html
- [48] M. Usman, “E. Shashi Menon Gas Pipeline Hydraulics CRC Press”, Accessed: May 13, 2025. [Online]. Available: https://www.academia.edu/38425144/E_Shashi_Menon_Gas_Pipeline_Hydraulics_CRC_Press
- [49] H. H. Bengtson, “Natural Gas Pipeline Flow Calculations”.
- [50] “Universal Gas Constant | GeeksforGeeks.” Accessed: May 13, 2025. [Online]. Available: <https://www.geeksforgeeks.org/universal-gas-constant/>
- [51] E. S. Menon, *Gas Pipeline Hydraulics*, 0 ed. CRC Press, 2005. doi: 10.1201/9781420038224.
- [52] F. D. S. Alves, J. N. M. D. Souza, and A. L. H. Costa, “Multi-objective design optimization of natural gas transmission networks,” *Comput. Chem. Eng.*, vol. 93, pp. 212–220, Oct. 2016, doi: 10.1016/j.compchemeng.2016.06.006.
- [53] “(PDF) PRESSURE DROP IN PIPELINES TRANSPORTING COMPRESSED HYDROGEN GAS,” ResearchGate. Accessed: May 07, 2025. [Online]. Available: https://www.researchgate.net/publication/370829586_PRESSURE_DROP_IN_PIPELINES_TRANSPORTING_COMPRESSED_HYDROGEN_GAS

APPENDIX

The scripts used for **modelling** are available [here](#)
While the **load data** files can be found [here](#)